On the petrology and microstructures of small-scale ductile shear zones in granitoid rocks: an overview

Alberto Ceccato[1*], Philippe Goncalves[2], Luca Menegon[3]

[1] Structural Geology and Tectonics Group, Geological Institute, Department of Earth Sciences, ETH Zurich, Sonneggstrasse 5, 8092 Zurich, Switzerland

[2] Laboratoire Chrono-Environnement, CNRS – Université de Bourgogne-Franche-Comté, 16 route de Gray, 25030 Besançon, France

[3] The Njord Centre, Department of Geosciences, University of Oslo, Postbox 1047 Blindern, 0316 Oslo, Norway;

*Corresponding author: aceccato@erdw.ethz.ch

Abstract.

Since the pioneering works of John Ramsay in the 1970's and 1980's, the analysis of exceptional exposures of small-scale shear zones (i.e. 10^{-3} – 10^{-1} m thick) in granitoid rocks provided invaluable insights into the processes controlling strain localisation in the middle and lower continental crust. Indeed, recent advancement in field, microstructural and petrological analyses of such small-scale shear zone have shed new light on the metamorphic, tectonic and fluid conditions promoting shear zone nucleation and development in granitoid rocks. In this paper we provide an overview of these new insights, comparing and integrating the results obtained from field, and microstructural and petrological analyses of small-scale shear zones in granitoid plutons and meta-granitoids from the Alps. A review of the deformation temperature shows that the granitoid shear zones development occurs between 350 to 600°C, with most of them localising in a restricted temperature window between 450 and 500°C. At these conditions, the magmatic assemblage is metastable and subjected to a series of metamorphic reactions. Furthermore, the development of shear zone does not occur under-closed system conditions. Introducing or expelling fluids and mass (i.e. metasomatism) during deformation has mineralogical consequences that control the rheology and the way shear zone evolves. Among the main mineralogical and microstructural changes, the breakdown of magmatic

feldspar(s) into fine-grained aggregates steers both the rheology and fabric evolution of shear zones in granitoid rocks, triggering further mechano-chemical feedback mechanisms. Future research should consider the occurrence of feedback processes between deformation, metamorphic and metasomatic processes to understand and quantify the evolution with time and strain of shear zone geometry and rheology, as well as of the development of larger-scale shear zone networks.

Keywords

Small-scale shear zones; Strain localisation, Granitoid rocks, Microstructure; Fluid-rock interaction.

1. Introduction

The seminal paper by Ramsay and Graham (1970) has formalised the concept of localised shear zone as a tabular-shaped zone of high strain. The shear zone they described is typically characterized by the occurrence of a strain-induced foliation with a sigmoidal-shaped geometry reflecting the symmetric decrease of strain from the centre to the boundary of the shear zone (Fig. 1a-b). The inferences of Ramsay and Graham about ductility and strain softening processes controlling shear zone development (*"[…] the structure in them appear to have been produced by ductile flow of the rock within the zone. […] Why then should the deformation become localized in these narrow zones? Perhaps it is because the initially deforming material became "strain softened" so that it acquired a progressively decreasing yield strength or higher ductility as the progress of deformation led to changes in its internal fabric."*) have inspired researchers for many years afterwards. Ramsay (1980) linked quantitatively the geometry of shear zones (quantified by φ, which represents the angle between the normal to the shear plane and the inclination of the strain marker) to the amount of shear strain γ, through the equation (Fig. 1c):

$$\gamma = \tan \varphi.$$

This equation effectively served as a pivotal link between data from field analyses, microstructural observations, experimental rock deformation and numerical and analytical modelling. Therefore, this quantitative approach laid the foundations for the multidisciplinary analysis of strain localisation processes at the meso- to micro-scale, leading to the development of the modern concept of (ductile) shear zone (Fossen and Cavalcante, 2017).

Ramsay developed important concepts on shear zone formation from field analysis of small-scale shear zones of cm-dm thickness within the meta-granitoid Maggia nappe (Central Alps, Fig. 1a) and the gabbroic rocks of Castell Odair (North Uist) (Ramsay and Graham, 1970). Indeed, meta-granitoid

units and granitoid plutons represent ideal natural laboratories for investigations of strain localization within macroscopically homogeneous and isotropic rocks, providing spectacular field exposures of shear zones and (incipient) shear zone networks (e.g., Ramsay and Allison, 1979; Ingles et al., 1999; Pennacchioni, 2005; Pennacchioni and Mancktelow, 2007; Pennacchioni and Zucchi, 2013; Ceccato and Pennacchioni, 2018).

In this paper, we report the recent advancements on the understanding of the microstructural processes controlling the nucleation and development of small-scale ductile shear zones in granitoid rocks. Such small-scale shear zones preferentially develop at retrograde metamorphic conditions at the transition between amphibolite to greenschist facies. However, small-scale shear zones similar to those described in the Maggia nappe have been also reported from different rock types and metamorphic conditions (e.g. granulite and eclogite facies in granitoid and gabbroic rocks: Van Roermund et al., 1978; Austrheim, 1987; Pennacchioni, 1996; Getsinger et al., 2013; Smith et al., 2015; Macente et al., 2017; Lee et al., 2022). Field analysis has highlighted the role of precursor brittle structures and compositional heterogeneities in controlling ductile strain localisation (Segall and Simpson, 1986; Bürgmann and Pollard, 1994; Christiansen and Pollard, 1997; Guermani and Pennacchioni, 1998; Pennacchioni, 2005; Fusseis et al., 2006; Pennacchioni and Mancktelow, 2007, 2018; Schrank et al., 2008b, Pennacchioni and Zucchi, 2013). Recent analytical and modelling advancements have provided new (semi-)quantitative insights on the role of microstructural and metamorphic processes in controlling the evolution of both the internal fabric and the yield strength of the deforming rock (e.g., Smith et al., 2015; Gardner et al., 2017; Meyer et al., 2016). In particular, the systematic investigation of deformation microstructures with electron backscatter diffraction (EBSD) and quantitative image analysis has allowed to constrain the microstructural and crystallographic signatures of specific deformation mechanisms and metamorphic reactions controlling strain accommodation (Menegon et al., 2008a,b; Pennacchioni et al., 2010; Kilian et al., 2011; Oliot et al., 2014; Spruzeniece and Piazolo, 2015; Ceccato et al., 2017, 2018; Gilgannon et al., 2017). Similarly, micro-analytical techniques (electron probe micro analyser – EPMA,

cathodoluminescence – CL, secondary ion mass spectrometer – SIMS, Fourier-transform infrared spectroscopy – FTIR; micro-computerized tomography – μCT) coupled to petrological modelling (phase diagram section calculation, geothermobarometry) allowed the role of reaction processes and fluids (mainly H_2O) in controlling the rheology and microstructural evolution to be identified (Kronenberg and Wolf, 1990; Oliot et al., 2010; Goncalves et al., 2012; Bestmann and Pennacchioni, 2015; Finch et al., 2016; Macente et al., 2017; Ceccato et al., 2020, 2022; Kronenberg et al., 2020). In addition, numerical and analytical models allowed to test inferences retrieved from field and microstructural analyses and to quantify the effect of deformation-metamorphism-metasomatism feedback processes on the geometry and rheology of shear zones (Mancktelow, 2002; Shrank et al., 2008; Huet et al., 2014; Ceccato et al., 2018; Kaatz et al., 2021). These new insights questioned existing models of purely strain-driven shear zone development (Ramsay and Graham, 1970; Ramsay, 1980; Lamouroux et al., 1994; Means, 1995). Indeed, recent studies have highlighted the role of both inherited and dynamically evolving (strain-dependent) gradients of fluid-rock interactions in controlling shear zone nucleation and development (Oliot et al., 2014; Pennacchioni and Mancktelow, 2018; Kaatz et al., 2021).

In this paper, starting from the concepts developed by John Ramsay and co-authors in the 1970', we provide a brief overview and an integrated critical discussion of the improvements that innovative approaches have brought to our understanding of the mesostructural, microstructural and petrological processes controlling the development of small-scale shear zones in granitoid rocks. This work aims to complement and expand the review work of Pennacchioni and Mancktelow (2018) on small-scale shear zones developed in granitoid rocks. For what regards the development of multiscale shear zones in general, the reader is addressed to more comprehensive and extensive reviews (e.g., Fossen and Cavalcante, 2017). Finally, we highlight several topics that still require further research efforts and provide some hints for further research development.

2. Field analyses of the meso-scale geometry of shear zones in granitoid rocks

The geometrical model of the ductile shear zone proposed by Ramsay and Graham (1970) allows to quantify the amount of shear strain accommodated across a shear zone from the deformation geometry (Fig. 1c). The model was based on the field analysis of small-scale (cm-dm thick) ductile shear zones developed within isotropic, homogeneous rocks (Fig 1a). In addition, it formalized the occurrence of "strain markers" in shear zones, such as the inclined sigmoidal foliation, the gradual deflection of crosscutting geological structures (e.g., dykes) and passive distortion of initially subrounded, suitably sized objects (Ramsay and Allison, 1979; Ramsay, 1980). In particular, the quantitative geometrical description and recognition of strain markers allowed the acknowledgement and quantification of the dominant role of a simple shear component of deformation, over pure shear, during the development of ductile shear zones (Ramsay and Graham, 1970; Ramsay, 1980). Since then, the analysis of the field geometry of small-scale shear zones and meso-scale networks led to significant improvement in our understanding of, as well as opened new debates on: (1) the process of shear zone nucleation; (2) the strain history recorded with increasing displacement; (3) the propagation and networking of shear zones.

2.1.Nucleation and geometry of incipient shear zones.

Contrasting models on shear zone nucleation have been proposed. Based on theoretical, experimental, microstructural and numerical studies, shear zones nucleate "spontaneously" as the result of either thermal softening at large (km) scale (Fleitout and Froidevaux, 1980; Regenauer-Lieb and Yuen, 2003; Duretz et al., 2014; Kiss et al., 2019), or the interconnection of zones of concentrated high strain caused by micro-scale, point-like flaws in an otherwise isotropic, homogeneous medium (Ingles et al., 1999; Mancktelow, 2002; Holyoke and Tullis, 2006; Meyer et al., 2016). In contrast, field observations on granitoid rocks provide increasing evidence for the necessary occurrence of a tabular, meso-scale precursor structure (either a brittle fracture or a compositional/structural heterogeneity) to allow a shear zone to nucleate (Mancktelow and Pennacchioni, 2013; Wehrens et al., 2017; Pennacchioni and Mancktelow, 2018, and reference therein). It is worth noting that brittle fractures

can be sometimes associated with pseudotachylytes (frictional melt produced by seismic slip along faults in silicate rocks: Sibson, 1975), which are then exploited as precursors to small-scale ductile shear zones in granitoids (e.g., Passchier, 1982; Takagi et al., 2000; Sullivan et al., 2013).

Furthermore, field observations suggest the likely occurrence of a threshold dimension of the precursor structures at the meter to tens of meters scale, below which precursor structures are not exploited as site for ductile strain localization in meta-granitoids (Mancktelow and Pennacchioni, 2013) as well as in foliated metamorphic rocks (Fusseis and Handy, 2008). The geometry of the precursor has a two-fold effect on the finite strain geometry of the shear zone (Mancktelow and Pennacchioni, 2005; Pennacchioni, 2005): (i) it determines the spatial extent (length) of the finite shear zone, and (ii) it controls the geometry (thickness, continuous vs. discontinuous) of the finite strain gradient. These observations have had important implications for the understanding of the processes controlling the growth of shear zones in both thickness and length, as well as networking, during strain accommodation.

2.2.Finite strain gradients and shear zone history

The symmetric, continuous decrease of shear strain from the core to the boundary represented by the sigmoidal foliation was interpreted to reflect the evolution through time and space of the rheology during strain localisation at constant temperature and pressure conditions (Ramsay and Graham, 1970; Schrank et al., 2008a,b). This interpretation has led previous authors to the formulation of some idealised models of shear zone, either narrowing or thickening with increasingly accommodated displacement (Type I-II-III-IV) (Hull, 1988; Means, 1995; Schrank et al., 2008b; Vitale and Mazzoli, 2008; see Fossen and Cavalcante, 2017 for a detailed discussion of such models). Such models generally include three different classes of shear zones (e.g., Means, 1995): (i) thickening shear zones in which the width increases with increasing displacement, usually related to strain-hardening rheology within the shear zone; (ii) narrowing shear zones in which the width decreases with increasing displacement, usually related to the occurrence of strain-softening rheology within the

shear zone; (iii) constant-width shear zones in which the width remains constant with increasing displacement. However, so far, no systematic and general relationship between accommodated displacement and thickness of ductile shear zone has been found (e.g., Fossen and Cavalcante, 2017). The datasets of thickness-displacement data are scattered and mainly limited to the small-scale ($\leq$ 10 m thick). These scattered data generally describe a not-better-defined trend of thickening with increasing accommodated displacement (Fig. 2; Fossen and Cavalcante, 2017). However, the concept itself of shear zones thickening contrasts with the concept of strain localisation *within* the shear zone, which would rather promote shear zone narrowing (Ramsay and Graham, 1970; Fossen and Cavalcante, 2017; Pennacchioni and Mancktelow, 2018).

In some cases, the finite thickness and the discontinuous/continuous character of the finite strain gradient might reflect the geometry of the compositional and rheological heterogeneity on which the shear zone nucleated (Mancktelow and Pennacchioni, 2005; Schrank et al., 2008b; Spruzeniece and Piazolo, 2015; Pennacchioni and Mancktelow, 2018; Kaatz et al., 2021). This interpretation is supported by thickness vs. displacement data retrieved from detailed field mapping, showing no systematic trends in shear zone thickness variation with (small, <1-10 m) displacement (Pennacchioni and Mancktelow, 2018). At larger (m to tens of meter) widths, and at larger shear strains, strain gradients around shear zones are commonly associated with an effective gradient in fluid-rock interaction and mass transfer (Marquer et al., 1985; Fourcade et al., 1989; Tobisch et al., 1991; Früh-Green, 1994; Barnes et al., 2004; Keller et al., 2004; Oliot et al., 2014; Finch et al., 2016; Kaatz et al., 2021). These multiscale observations suggest that the analysis of the development and the role of such fluid gradients may be key to improve our understanding of the evolution of shear zone thickness during shearing. Indeed, recent theoretical and numerical models considering fluid expulsion related to chemo-mechanical pressure gradients induced by rheological and chemical contrasts during shear zone development reproduce and nicely explain the pattern of shear zone evolution and networking inferred from field observations of multiscale shear zone networks in crystalline rocks in general (e.g., Oliot et al., 2014; Finch et al., 2016; Kaatz et al., 2021). Therefore, even though widely accepted

and adopted to interpret shear zones geometry and rheology, the standard classification of thickening-narrowing-constant thickness shear zones might oversimplify the complex (and possibly cyclical) thickening-narrowing and rheological history recorded in shear zones during displacement accommodation (e.g., Steffen et al., 2001; Schrank et al., 2008b).

2.3.Insights into shear zone growth and networking

Granitoid rocks commonly display well-exposed outcrops of multi-scale shear zone networks, presenting shear zones ranging from 10^{-4} m to 10^{5} m in length (Fossen and Cavalcante, 2017). Despite the overall agreement on the theoretical process of formation of interconnected shear zone network through the coalescence of single, isolated shear zones, the geologic process controlling linkage and actual coalescence remains matter of debate (Carreras et al., 2010; Fossen and Cavalcante, 2017). A network of pre-existing compositional and structural heterogeneities within an otherwise homogeneous granitoid rock could provide the seed on which a shear zone network develops, controlling the incipient stages of shear zone formation and networking (Pennacchioni and Mancktelow, 2007). However, the mechanisms controlling the formation of large scale, complex networks formed by shear zones of different width and length remains matter of debate.

Especially when shear zones nucleate from brittle precursors, contrasting models have been proposed to explain the transition from isolated, small-scale shears to meso-scale interconnected networks (Fusseis et al., 2006; Pennacchioni and Mancktelow, 2007; Fusseis and Handy, 2008; Schrank et al., 2008). Detailed field mapping of incipient meso-scale networks in meta-granitoids has shown that, at least for small values of accommodated shear strain, the shear zone length is limited to the length of the precursor structure. In the latter case, the shear zone did not appear to extend in length with increasingly accommodated strain, as it has been inferred from the preservation of contractional jogs at the tip of sheared precursor structures (Pennacchioni, 2005; Pennacchioni and Mancktelow, 2007; Pennacchioni and Zucchi, 2013). On the other hand, based on microstructural and meso-scale observations in foliated meta-pelites of Cap de Creus, Fusseis et al. (2006) proposed that small-scale

shear zones can grow laterally following the synchronous propagation of the migrating brittle precursor tip parallel to the shear plane in the shear direction. Reaction-induced softening of the host rock around the shear zones, triggered by fluid diffusion during shearing, may provide another feasible way to extend and widen single shears which will invariably connect into a complex network with increasing strain (e.g., Oliot et al., 2014; Kaatz et al., 2021).Therefore, several processes might be responsible for shear zone networking, and both metamorphic, ductile and brittle-ductile processes need to be considered to understand the processes of shear zone growth in time and space (e.g., Schrank et al., 2008b, Nevitt et al., 2014; Nevitt and Pollard, 2017; Nardini et al., 2018; Döhmann et al., 2019).

3. Petrological constraints on shear zone development in granitoid rocks

Shear zones are the loci of numerous interactions between deformation, metamorphism and fluid flow. For instance, the development of shear zones in granitoid rocks is concomitant with mineralogical changes that, in most cases, favour strain softening and localisation (McCaig, 1984; Gueydan et al., 2003; Holyoke and Tullis, 2006). In turn, deformation enhances metamorphic reactions either by overcoming kinetic barriers or by favouring the development of permeability and fluid infiltration (Fusseis et al., 2009; Oliot et al., 2014). Understanding the feedbacks between all these interdependent processes is critical to better model strain localisation.

In general, metamorphic reactions may be driven by: (i) change in pressure (*P*)-temperature (*T*) conditions, (ii) change in fluid content and composition (*fl*), (iii) change in bulk chemistry (*X*) due to mass transfer (i.e. metasomatism). During deformation of a granitoid rock, it is very likely that the magmatic assemblage is metastable at the *P-T-fl-X* conditions of the deformation (Goncalves et al., 2012). In this case, metamorphic and metasomatic reactions are also driven by (iv) disequilibrium and the equilibration of the metastable magmatic assemblage at the *P-T-fl-X* conditions of the deformation (Goncalves et al., 2012). In the following section, we review phase relations of granitoid

rocks as a function of *P-T-fl-X* conditions and discuss their influence on strain localisation and shear zone development through the analysis of *P-T*, *T-*M_{H2O} and *T-X* phase diagram sections. Phase diagrams were computed with Perple_X 6.9.1 (Connolly, 2005) for the bulk composition of an average meta-granodiorite from the Neves Lake area (e.g., Leydier et al., 2019), using the thermodynamic database of (Holland and Powell, 2011; TC-DS62) and the a-X solid solution models of White et al. (2014). The chemical system includes K_2O-FeO-MgO-Al_2O_3-SiO_2-H_2O (KFMASH). MnO, TiO_2 and Fe_2O_3 are not considered here. Mineral abbreviations are from Whitney and Evans (2010).

3.1.P-T conditions of shear zones in meta-granitoids and granitoid plutons

Since the description of small-scale shear zones in the meta-granitoid unit of the Maggia Nappe of Ramsay and Graham (1970), many other occurrences of similar small-scale shear zones were reported from the crystalline basements and granitoid plutons of the Alps and other localities worldwide (Pennacchioni and Mancktelow, 2018, and reference therein). Despite the different tectonic and metamorphic history of (Alpine) meta-granitoid and magmatic plutons, all the reported cases of small-scale shear zones developed between 350 °C and 600 °C, during cooling of the pluton or during the retrograde *P-T* path of the meta-granitoid unit (Fig. 3a). In detail, shear zone nucleation and development in meta-granitoid units occurred mainly at $P > 0.4$ GPa and T = 420-600 °C (light blue areas in Fig. 3a). In granitoid plutons, emplaced at middle and upper crustal levels, shear zone nucleation occurred at $P < 0.5$ GPa and T = 350-550 °C (pale orange areas in Fig. 3a), similarly to what was already reported by Gapais (1989). Overall, these data show that small-scale shear zones in meta-granitoids preferentially develop in a restricted *T* window at the transition between amphibolite and greenschist facies. The main differences between shear zones developed in meta-granitoid units and those from cooling granitoid plutons probably reside in (i) the timescale of deformation (much shorter for cooling plutons) and (ii) fluid (mainly H_2O) availability, which has enormous effects for the rheology, metamorphic processes and longevity of shear zones (see sections below).

3.2.P-T phase relations of granitoid systems under H_2O-saturated conditions

We explore, through phase relation modelling, the main mineralogical changes expected at the conditions of shear zone development as defined above. Figure 3b-c shows the *P-T* phase diagram sections computed for the KFMASH system, which is suitable to model the main phase relations in granitoid systems. Here, we firstly consider phase relations calculated at H_2O-saturated conditions for the sake of simplicity, and then we discuss the effect of H_2O-undersaturation on phase relations in granitoid rocks in the next Sections (see below). Figure 3b shows that from ca. 700 °C (i.e. the temperature of the hydrated solidus) to about 550 °C and a pressure from 0.1 to 0.8 GPa, there is a large multivariant field that consists of Pl + Bt + Qz ± Amp ± Kfs corresponding to the expected magmatic assemblage for a granodiorite. During cooling of a pluton or a retrograde path, there are no major mineralogical changes from 700 to 550 °C. In contrast, between 450 and 500 °C, the phase diagram shows several phase boundaries that are mostly related to a main univariant reaction (1) in the KFMASH system:

$$Pl + Kfs + Bt + Qz + H_2O = Ms + Chl + Ab + Ep \quad (1)$$

that separates amphibolite and greenschist facies. For the average granodiorite bulk composition, there are four divariant reactions associated with reaction (1). Among them, we discuss two divariant reactions located at pressure above 0.5 GPa that account for the main mineralogical changes observed in granitoid shear zones:

$$Kfs + Bt + Pl + Qz + H_2O = Ab + Ep + Ms \quad (\mathbf{Chl})$$

$$Pl + Bt + Qz + H_2O = Ms + Chl + Ep \quad (\mathbf{Kf})$$

These two divariant reactions occur in a narrow temperature window, between 450 °C and 500 °C (Fig. 3c), and they can be linked with classic petrological observations made in shear zones: (a) the saussuritisation of magmatic plagioclase into a fine grained assemblage consisting of albite, epidote and muscovite (e.g., (Fitz Gerald and Stünitz, 1993; Stünitz and Fitz Gerald, 1993; Oliot et al., 2010;

285 Goncalves et al., 2012; Menegon et al., 2008a) (b) the breakdown of K-feldspar to produce muscovite
286 (Hippertt, 1998; Gueydan et al., 2003; Tschegg and Grasemann, 2009); and (c) the formation of
287 muscovite and chlorite at the expense of biotite (Goncalves et al., 2012; Airaghi et al., 2020).
288 Additionally, myrmekite formation at the expense of K-feldspar is another commonly reported
289 reaction which contributes to the development of shear zones in granitoid rocks in this temperature
290 window (Tsurumi et al., 2003; Menegon et al., 2006; Ceccato et al., 2018; Cisneros-Lazaro et al.,
291 2019).

292 To conclude, the breakdown of the magmatic load-bearing framework (LBF; Handy, 1990) of Pl +
293 Qz ± Kfs (almost ~85% of the rock volume) into a fine-grained assemblage consisting of Ab + Ms +
294 Ep ± Chl is a first order softening mechanism that may favour strain localisation. Thus, in granitoid
295 rock, the 450-500 °C temperature range corresponds to the most favourable conditions for the
296 initiation of reactions promoting strain localisation. The identified temperatures provide the
297 maximum temperatures at which such reactions may occur. Any occurrence of strain localization and
298 shear zone formation below these temperatures might be effectively controlled by the same
299 parageneses.

300 *3.3.Fluid (H_2O) saturation and mineralogical effects*

301 In the previous section, the phase relations have been investigated assuming H_2O-saturated conditions
302 during deformation. However, H_2O-saturation might not even be the case or persist during the whole
303 history of shear zone development, as it has been suggested by several recent studies (Finch et al.,
304 2016; Ceccato et al., 2020; Menegon and Fagereng, 2021). Thus, we investigate here the role of H_2O
305 content, and more particularly H_2O undersaturation on phase relations. Figure 3d is a T-M_{H2O} phase
306 diagram computed at a constant pressure of 0.6 GPa. The black dashed curve traces the boundary
307 between H_2O-saturated (to the right) and H_2O-undersaturated (to the left) phase assemblages. The T-
308 M_{H2O} diagram shows that the meta-granodiorite composition is rather sensitive to very little changes
309 in M_{H2O} at undersaturated conditions. Indeed, M_{H2O} varies overall from 1.2 to 6 mol (0.33 to 1.63

wt%). Conversely, at H_2O-saturated conditions, the mineral assemblage is mainly dependent on the temperature. During deformation and cooling from 550 to 400 °C, the amount of H_2O in mol per kilogram of rock must increase by more than 160% to keep the assemblage H_2O-saturated. The main mineralogical effects of H_2O-undersaturation are (1) the stabilization of garnet, (2) the increase of plagioclase stability to lower temperature (485 to 450°C) and (3) the breakdown of chlorite. Under closed-system conditions (no gain and loss of H_2O), cooling from 550 °C and deformation would result in the formation of garnet-bearing, at intermediate degrees of under-saturation, or even kyanite bearing shear zones for very low (geologically unrealistic) H_2O contents and low temperature (M_{H2O} < 0.12 mol, T < 425 °C). The stabilization of garnet and kyanite may be due also to bulk composition effects (abundant MnO and Fe_2O_3 for garnet), or extensive mass-transfer at fluid-saturated conditions (e.g., kyanite-bearing, granitoid-derived micaschists reported by Sassier et al., 2006). Nonetheless, the occurrence of such index minerals could suggest shear zone formation at H_2O under-saturated conditions. At intermediate stages of H_2O-undersaturation, i.e. in which a fluid is available but not enough to result in H_2O as a free-fluid phase, metamorphic parageneses containing progressively more proportions (in terms of both modal quantity and number of different phases) of hydrated minerals will be stabilised. Then, after H_2O saturation, the availability of H_2O as a free-fluid phase has enormous effects on the kinetics of metamorphic reactions (having H_2O as limiting reactant) and fluid-assisted deformation processes (e.g., dissolution-precipitation and mass transfer, e.g., Yardley and Valley, 1997; Wintsch and Yi, 2002; Ceccato et al., 2020; Tursi, 2022). Therefore, H_2O-saturation conditions directly affects the bulk rheology, and need to be investigated in detail for a thorough understanding of shear zone formation and evolution.

3.4.Fluid conditions during shear zone development

H_2O-saturation conditions, and thus the occurrence of a free-fluid phase, may be affected by several parameters of the geological setting in which granitoid shear zones develop. Indeed, initial fluid availability, the supply rate from any (either internal or external) fluid source, the retrograde cooling rate of the (meta-)granitoid and the occurrence of retrograde hydration metamorphic reactions may

336 determine the fluid-saturated vs. -undersaturated conditions of the system regardless of the "open vs.
337 closed" conditions of the system with respect to fluid flow (e.g., Yardley, 1981).

338 A variable fluid behaviour during shear zone development can be inferred from field, microstructural
339 and petrological evidence. When small scale shear zone in granitoid rocks exploit precursor
340 structures, common precursors are: (i) mineralized joints; (ii) veins; (iii) alteration haloes due to fluid-
341 rock interaction along the selvages of brittle fractures and veins (e.g., Mancktelow and Pennacchioni,
342 2005; Pennacchioni, 2005). This set of precursor types involves the occurrence of (mineralising)
343 fluids during at least the formation of the precursors, and thus, local fluid-saturated conditions. Many
344 case studies report that, during precursor formation, the fluid is likely to be of local origin and the
345 granitoid rock behaves as a closed system (e.g., Cesare et al., 2001; Pennacchioni, 2005;
346 Mittempergher et al., 2014; Leydier et al., 2019; Ceccato et al., 2020). After precursor nucleation,
347 phase diagram section calculations have shown that incipient shearing on small-scale shear zones
348 may occur at both fluid-saturated (e.g., in meta-granitoid rocks of the Neves Lake area, Leydier et al.,
349 2019) and fluid-undersaturated conditions (e.g., shear zones from the Adamello, Rieserferner and
350 Sierra Nevada granitoid plutons, Ceccato et al., 2020). In addition, isotopic and major element
351 chemical analyses suggest that, at least within granitoid plutons, the incipient stages of shearing as
352 well might occur at closed system conditions (Pennacchioni, 2005; Mittempergher et al., 2014). At
353 larger-scale, (m to tens of m in width) shear zones in meta-granitoid rocks deform under fluid-
354 saturated, open-system conditions, commonly accompanied by significant mass transfer (e.g.,
355 Marquer, 1985; Fourcade et al., 1989; McCaig et a., 1990; Früh-Green, 1994; Barnes et al., 2004;
356 Rossi et al., 2005; Goncalves et al. 2012; Oliot et al., 2014; Rolland and Rossi, 2016; Wehrens et al.,
357 2017). At such large scale, given the paucity of connate fluids in (meta-)granitoid rocks, an external
358 fluid source is needed, as it is commonly reported for other large-scale, retrograde orogenic shear
359 zones (e.g., Kuckaus shear zone, Diener et al., 2016). As already proposed by Fourcade et al. (1989),
360 the development of a network of shear zones "well-interconnected" among them, and connected to
361 an external fluid source, likely promote fluid-flow, open system conditions and significant mass-

362 transfer (see below; e.g., Oliot et al., 2014). However, this topic deserves further investigations and
363 research.

364 *3.5. Mass transfer and metasomatism in shear zones*

365 Shear zones developed under fluid-saturated conditions are also likely affected by mass transfer either
366 via diffusion or infiltration metasomatism (Korzhinskii, 1970). Metasomatic reactions result in
367 mineral assemblages that differ significantly from those formed where the system is either open or
368 closed to only H_2O transfer. Mass transfer (i.e., metasomatism) has been reported and quantified in
369 many granitoid shear zones (e.g., Goncalves et al., 2012 and reference therein). Although each shear
370 zone should be treated as a unique case (e.g., Tursi et al., 2018), granitoid shear zones developed
371 under greenschist to amphibolite facies conditions show very consistent mass transfer with, in
372 general, a gain in MgO and H_2O coupled with a loss of Na_2O and CaO (Goncalves et al., 2012). It is
373 beyond the scope of this contribution to explain this coupling, but we explore via phase relation
374 modelling the effect of this specific mass transfer on the mineralogical composition of granitoid shear
375 zones. Based on the literature review, we propose a hypothetical mass transfer scenario, with only
376 four mobile components: gain of H_2O and MgO coupled with the loss of CaO and Na_2O. Mass transfer
377 evolves linearly from the protolith composition to a metasomatic shear zone characterized by +200%
378 for MgO and -100% and -75% for Na_2O and CaO respectively. The amount of H_2O is computed such
379 that the system is kept H_2O saturated. The phase diagram is computed at 0.6 GPa.

380 The change in bulk composition induced by mass transfer has no effects on the absolute *P*-*T* position
381 of the (**Chl**) and (**Kf**) reactions (Fig. 4a). At 0.6 GPa, these reactions are located at 480-485 °C (Fig.
382 4a). Under closed system conditions (X=0, Fig. 4b), no major mineralogical changes occur before
383 reaching the (**Chl**) and (**Kf**) reactions. At 485-480 °C, 65 vol% of the rock (Pl and Kfs) is
384 recrystallized into fine-grained aggregates of Ab + Ep (~55%) ± phyllosilicates (Bt + Ms, ~20%).
385 Figures 4a-4c show the effect of mass transfer at a temperature of 475 °C just below the onset of shear
386 zone development. Progressive mass transfer induces a continuous breakdown of Ab + Ep to produce

large amounts of Ms + Chl + Qz, (Fig. 4c). In a strongly metasomatized system (X=1), the resulting rock in the shear zone would be a phyllonite consisting of 50% of Qz and 50 % of Ms + Chl (Fig. 4c).

Therefore, the main result of mass transfer and metasomatic reactions in shear zones is the progressive replacement of the protolith feldspars building up the LBF (Handy, 1990). This results in softening of the deforming shear zone (Gueydan et al., 2003; Oliot et al., 2014). The formation of fine-grained aggregates of Ab + Ep at intermediate degrees of metasomatism first, and then the stabilization of large amounts of phyllosilicates (Bt + Ms + Chl) at advanced stages, have enormous effects on the rheology and fabric development of shear zones, leading to progressive softening and foliation development.

4. Shear zone microstructure and rheology

The "strain softening mechanisms" proposed by Ramsay and Graham (1970) involve the modification of the spatial arrangement, geometrical characters, chemical composition and phase proportions of the mineral constituents at the micro- to meso-scale (e.g., Poirier, 1980; White et al., 1980).

4.1.Microstructural processes and rheological effects

At the temperature conditions at which small-scale shear zones are inferred to nucleate and develop (350-600 °C), strain accommodation and the development of the shear zone fabric involve grain-size reduction (GSR) of mineral phases (Ramsay and Allison, 1979). GSR in quartz is mainly accommodated by dynamic recrystallization (Stipp et al., 2002; Bestmann and Pennacchioni, 2015); whereas feldspars undergo predominantly brittle GSR (Ree et al., 2005; Viegas et al., 2016) in addition to the retrograde metamorphic reactions described above (Fig. 5a-b). The contribution of dynamic recrystallisation to GSR in feldspars is negligible in the temperature range considered here (Gapais, 1989; Fitz Gerald and Stünitz, 1993; Menegon et al., 2008b).

Associated with GSR processes, especially when local mass-transfer is involved, phase mixing (PM) may result from neo-crystallisation and phase nucleation related to metamorphic reactions or to the

emergence of synkinematic porosity (Fusseis et al., 2009; Kilian et al., 2011; Menegon et al., 2015; Ceccato et al., 2018; Gilgannon et al., 2020, 2021) (Fig. 5a-b). The main result of GSR and PM processes consists in the formation of fine-grained, mixed polyphase aggregates characterised by a rheology (i.e., deformation mechanisms) "weaker" than that of the parent mineral phases (Kilian et al., 2011; Platt and Behr, 2011a,b; Sullivan et al., 2013; Wehrens et al., 2016; Mansard et al., 2018; Stenvall et al., 2019). Indeed, fine-grained, polyphase aggregates preferentially deform by grain-size sensitive (GSS) creep processes, including grain-boundary sliding (GBS) and diffusion creep, which are inherently characterised by a "weak" linear-viscous rheology (Fig. 5c). However, the softening potential of GSR by dynamic recrystallisation of monomineralic aggregates is limited by the piezometric relationships and the balance between grain size reduction and crystal growth processes (De Bresser et al., 2001; Cross et al., 2015; Tokle and Hirth, 2021) (Fig. 5d). Effective softening is mainly related to the combined activation of GSR and PM processes resulting in polyphase aggregates (Kilian et al., 2011; Spruzeniece and Piazolo, 2015; Ceccato et al., 2018; Stenvall et al., 2019). Indeed, the polyphase mixed nature and fine grain size of these aggregates have two major consequences on the kinetics of rheology-controlling deformation mechanisms (Herwegh et al., 2011): (i). the fine grain size enhances the efficiency of diffusion-assisted creep processes (Coble creep, dissolution-precipitation creep) through the reduction of the diffusion length scales; (ii) PM hinders the efficiency of crystal growth by pinning, maintaining the overall grain size of the polyphase aggregates in the range where diffusion-assisted GSS creep is dominant (Fig. 5d). Therefore, GSR and PM are the key processes steering the evolution of shear zone strain-softened rheology, as well as of the shear zone micro- and meso-scale fabric. Whilst the strength of mono-phase aggregates can be estimated by paleopiezometers for dislocation creep (e.g., for quartz, Cross et al., 2017), the strength of polyphase mixed aggregates is still poorly constrained and requires the adoption of analytical mixing models under significant assumptions (Huet et al., 2014; Platt, 2015). Nevertheless, rheological mixing models can be very effective in the quantification of softening related to PM processes (e.g., Fig. 5c; Huet et al., 2014; Gerbi et al., 2016; Ceccato et al., 2018).

4.2.Fabric and microstructural development

Progressive GSR with increasing strain and metamorphic reactions lead to the development of fine-grained, recrystallized aggregates. These aggregates progressively merge, with increasing strain, to form the typical strain-dependent foliation observed along the ductile shear zone walls, leading to the transition from protomylonite, to mylonite and ultramylonite (Ramsay and Allison, 1979; Ramsay, 1980; White et al., 1980) (Fig. 1c). In particular, the development of the characteristic sigmoidal foliation of protomylonites is primarily controlled by the formation of a phyllosilicate-dominated interconnected weak layer (IWL) microstructure during the incipient stages of deformation (e.g., Handy, 1990; Holyoke and Tullis, 2006). With increasing strain, this phyllosilicate dominated IWL is however overtaken and disrupted by the development of an IWL microstructure formed by coalesced fine-grained, polyphase aggregates resulting from feldspars breakdown and neo-crystallisation (Hippertt and Hongn, 1998; Stenvall et al., 2019). As strain accommodation, coalescence and phase mixing progress, fine-grained homogeneous polyphase ultramylonites form, representing the final product of strain accommodation and rheological softening (Ramsay and Allison, 1979; Kilian et al., 2011; Cross and Skemer, 2017; Stenvall et al., 2019) (Fig. 6a). Thus, the strength and textural evolution of ductile shear zones strictly depend on the fate of feldspar phases, forming the LBF in the protolith (Handy, 1990) (Fig. 6a). As described above, the dismantling of the feldspars-LBF is deeply affected by the H_2O-saturation conditions of the system and the occurrence of mass-transfer processes, which in turn affect the final ultramylonitic mineral assemblage.

4.3.Deformation mechanisms and fluids

Aqueous fluids are agents of chemical (hydrolytic) softening in nominally anhydrous minerals (e.g., Kronenberg and Wolf, 1990; Bras et al., 2021; Ceccato et al., 2022). Similarly, the occurrence of a fluid phase may enhance the kinetics of retrograde metamorphic reactions aiding strain localisation, then affecting the shear zone bulk rheology as well (e.g., Spruzeniece and Piazolo, 2015; Stenvall et al., 2020). Consequently, the evolution of both the bulk fluid content of shear zone and the intracrystalline fluid content of mineral phases have major effects on the geometrical and rheological

464 evolution of shear zones (Spruzeniece and Piazolo, 2015; Finch et al., 2016; Stenvall et al., 2020;
465 Kaatz et al., 2021).

466 In turn, the microstructural and rheological evolution of shear zone with increasing strain may affect
467 both the bulk fluid content of the shear zone and of its mineral constituents (Bestmann and
468 Pennacchioni, 2015; Finch et al., 2016). Indeed, fluid content may evolve with increasing strain as an
469 effect of feedback processes between deformation (GSR-PM), and metamorphic-metasomatic
470 processes (Hobbs et al., 2010; Oliot et al., 2014; Finch et al., 2016; Kaatz et al., 2021). Second-order
471 processes related to GSR may lead to both the release of intracrystalline fluids (e.g. fluid inclusions
472 and intracrystalline H_2O) into the shear zone, as well as to the drying up of the shear zones during
473 recrystallisation as a consequence of increased grain boundary area (Pennacchioni and Cesare, 1997;
474 Mancktelow and Pennacchioni, 2004; Bestmann and Pennacchioni, 2015). Furthermore, the
475 activation of GSS creep and PM processes has a two-fold effect on fluid content (Fig. 6b): (i) they
476 promote fluid flow toward the most strained portions of the shear zone through the development of
477 local grain-scale dilatancy (i.e., creep cavitation; Fusseis et al., 2009; Menegon et al., 2015;
478 Spruzeniece and Piazolo, 2015; Gilgannon et al., 2021); (ii) at the same time, the rheological contrast
479 between the weak shear zone and the undeformed host rock may lead to pressure gradients driving
480 fluids away from the shear zone toward the host rock (Mancktelow, 2006; Oliot et al., 2014; Finch et
481 al., 2016; Menegon and Fagereng, 2021). The relevance of all these processes may change depending
482 on the open vs. closed conditions of the system with respect to fluid flow, and upon the stabilization
483 of a stable retrograde metamorphic paragenesis (Yardley and Valley, 1997; Diener et al., 2016;
484 Stenvall et al., 2020). The rheology and geometry evolution of shear zones are therefore the results
485 of a delicate equilibrium between fluid availability and deformation-metamorphic-metasomatic
486 feedback processes at the microscale.

5. Final remarks and future directions

The analysis of meta-granitoid rocks provided very helpful inferences for the understanding of (incipient) strain localization processes in isotropic geological bodies at mid crustal conditions. Granitoid units, however, represent the exception rather than the rule for what regards the typical characters of metamorphic units in the continental crust and orogenic belts. The occurrence of pervasive heterogeneities (e.g., foliations) in metamorphic orogenic units, and the composition of such units themselves, might deeply affect the development of shear zones at general mid-crustal conditions (Rennie et al., 2013; Diener et al., 2016).

Small-scale shear zones in granitoid rocks predominantly nucleate exploiting precursor brittle structures and compositional heterogeneities. They nucleate and develop within a restricted temperature window (350-600°C), during the retrograde or cooling path from amphibolite to greenschist facies metamorphic conditions. At these conditions, the meta-stable granitoid mineral assemblage is affected by a series of retrograde divariant reactions that assist strain accommodation within the shear zones. These reactions are spatially restricted, i.e. localised, within shear zones (and not in the host rock in general), suggesting that metamorphic retrograde equilibration of the metastable assemblage is promoted by either fluid-rock interaction or deformation processes taking place within the shear zones.

These reactions mainly involve breakdown of feldspar(s) with the resulting development of either fine-grained polyphase or phyllosilicate-rich aggregates. Thus, feldspar breakdown at retrograde conditions controls the evolution of both the rheology (through the activation of GSS creep mechanisms) and the fabric (through the development of phyllosilicate- or polyphase-aggregate-bearing IWL) of shear zones. Indeed, shear zone rheology is controlled by the activation of GSS creep and PM processes, which result in the strain softening rheology inferred by Ramsay and Graham (1970). Such microstructural processes have a major role in controlling the diffusion of fluids and the

extent of metasomatic and retrograde metamorphic processes leading to host rock softening and shear zone widening.

Notwithstanding the improvements provided by detailed field, analytical and numerical studies, several points remain unclear and deserve further analyses. We think that three main topics should be at the core of future research on shear zone development and strain localisation in both granitoid rocks and the continental crust in general, including: (1) quantification of strain evolution and rheology; (2) understanding transient vs. steady state evolution; (3) integrated, multiscale shear zone networking models.

The first aspect consists in the quantification of rates and magnitudes (e.g., progression of recrystallisation with strain) of deformation processes in natural shear zones, in order to be then compared to the results of experimental rock deformation and numerical modelling. Field, microstructural and petrological integrated analyses should aim at the quantification of the effects of the feedbacks between deformation, metamorphism and metasomatism on the rates and intensity of strain localisation and on the strength of ductile shear zones. The integration of rheological mixing models with quantitative microstructural observations along strain/fluid gradients of small-scale shear zones will allow to quantify the effects of specific deformation, metamorphic and metasomatic processes on the bulk rheology of shear zones as a function of strain and of different degrees of fluid-rock interaction (Shigematsu, 1999; Gerbi et al., 2010; Cross and Skemer, 2019; Whyte et al., 2021). Both strain and fluid-gradients develop through time, and thus their analysis may provide fundamental insights into the evolution in time of microstructural processes, feedback mechanisms and rheology.

In addition, further investigations are necessary to understand the strict relationship between strain accommodation and the gradients of fluid-rock interaction intensity observed at various scale. Is there an effective transition from closed to open system with increasing strain and networking (Fourcade et al., 1989, Oliot et al. 2014)? What is the actual process controlling this transition?

These insights will in turn shed new light on other relevant questions: (i) what are the factors controlling the role of ductile shear zone as fluid pathways?, and (ii), what controls the evolution of the equilibrium between fluid intake and expulsion? Transient vs. continuous fluid intake and fluid flow is then reflected on the softening mechanisms controlling strain accommodation through time. This will have significant implications for the understanding of transient vs. steady-state character of deformation. Therefore, the final questions become: is strain accommodation in shear zones continuous or discontinuous (i.e., transient vs. steady state deformation)? What are the parameters controlling transient vs. steady state deformation? Further improvements on geochronological dating techniques may provide the necessary tools to address this question (Oriolo et al., 2018).

Considering the nucleation of shear zones on precursor structures, what are the boundary conditions that drive shear zone widening and networking? Do small-scale shear zones effectively represent the seeds of larger scale mylonitic belts? To what scale do brittle and compositional precursors control the nucleation of shear zones? The existing models for shear zone growth and networking still partially fail to integrate field, microstructural and petrological observations consistently. So far, thickness-length-displacement data retrieved from detailed mapping of networks of meso-scale shear zones do not show any systematic trend in shear zone thickness variation, neither at small-scale, nor connecting the small-scale toward the large scale (Fossen and Cavalcante, 2017; Pennacchioni and Mancktelow, 2018).

Recent results from field, microstructural and numerical analyses have highlighted the effects of scale-dependent feedback mechanisms in controlling the geometry and the networking of general shear zones in space and time (Regenauer-Lieb and Yuen, 2003; Schrank et al., 2008b; Hobbs et al., 2010, 2011; Mancktelow and Pennacchioni, 2013; Oliot et al., 2014; Finch et al., 2016; Meyer et al., 2016; Pennacchioni and Mancktelow, 2018; Kiss et al., 2019; Bras et al., 2021; Kaatz et al., 2021). Such feedback mechanisms largely originate from the interaction between deformation, mass transfer, chemical and heat diffusion (i.e. metamorphic and metasomatic) processes, which might take

561 place at different length- and timescales during shear zone evolution (Fig. 2; e.g., Regenauer-Lieb
562 and Yuen, 2003; Hobbs et al., 2010; Kaatz et al., 2021). Chemical diffusion and (metamorphic)
563 reactions seem to control the thickness of small- and meso-scale shear zones. For example, Oliot et
564 al. (2014) proposed a model for shear zone thickening and networking driven by fluid expulsion
565 (meso-scale mass transfer) from shear zones, triggered by chemically and mechanically induced
566 pressure gradients, with consequent metasomatic-softening reactions in the host rock. At larger scales
567 ($>10^3$ m), shear heating may contribute significantly to the softening of the host rock leading to shear
568 zone thickening (e.g., Kiss et al., 2019). The main result of such feedback mechanisms is the softening
569 of the host rock, which in turn would lead to shear zone thickening. At first sight, these softening-
570 driven model of shear zone thickening might seem to dispute the classical model of softening-
571 narrowing shear zones (e.g., Means, 1995). However, rather than considering softening within the
572 shear zone itself as the classical model does, such model expect softening in the host rock along the
573 selvages of the shear zone and shear zone tips, allowing more rock to be included in the deforming
574 shear zone during softening (Oliot et al., 2014).

575 During shear zone thickening and networking, the deforming systems may be subjected to different
576 feedback processes controlling both the deformation mechanisms and the rate at which strain is
577 accommodated (Schrank et al., 2008b; Hobbs et al., 2010; Meyer et al., 2016; Bras et al., 2021).
578 Therefore, we must consider these feedback mechanisms in the future studies that seek to explore the
579 processes of networking and mesoscale evolution, integrating field, microstructural and petrological
580 observations. These studies will need to be supported by an extended database of displacement vs.
581 thickness data retrieved from quantitative, multiscale mapping of shear zone networks on optimally
582 exposed outcrops. Accordingly, numerical models should aim at comparing their results with such
583 databases provided by field analyses.

584

Acknowledgments

We are deeply grateful to Neil Mancktelow and Giorgio Pennacchioni for inspiring discussions about shear zones over the past years and for their support during the writing of this paper. We thank Johann Diener and an anonymous reviewer for their comments on a previous version of the manuscript. This research did not receive any specific grant from funding agencies in the public, commercial, or not-for-profit sectors.

Figure captions

Figure 1. **(a)** Example of small-scale shear zone from the Ramsay's type locality close to Poncione dei Laghetti (Maggia nappe, Central Alps). Courtesy of Neil Mancktelow. **(b)** Example of small-scale shear zone from the Neves Lake area (Tauern Window, Eastern Alps). Courtesy of Giorgio Pennacchioni. **(c)** Schematic representation of the geometrical model of a Ramsay-type shear zone, showing the transition, developed along the strain gradient identified by the sigmoidal foliation (marked by grey dashed curves), from the undeformed granitoid host rock (HR), to protomylonite (Proto), mylonite (Myl) and ultramylonite (Umyl). The model presents the geometrical parameters (α, α', φ, θ) and equations adopted to calculate shear strain γ. The angles α and α' represent the angle between the shear plane and the orientation of a passive strain marker (e.g., an aplitic dyke, dark grey). Redrawn and modified after Ramsay (1980). T: thickness, D: displacement.

Figure 2. Thickness vs. Displacement diagram, redrawn from Fossen and Cavalcante (2017) including the data reported in Hull (1988(, Takagi et al. (2000) and Pennacchioni and Mancktelow (2018). The reader is referred to each of these publications for further details on the data. The transparent arrows suggest the likely Thickness-Displacement trends described by some datasets from different small-scale shear zone networks. At the bottom, the length scales for different diffusion (heat, fluids, mass) processes are reported (from Hobbs et al., 2011). The inset shows the theoretical Thickness-Displacement trends with the inferred softening-hardening rheology as proposed by the models of Means (1995).

Figure 3. *P-T-fl* conditions of shear zones development in the Alpine (and neighbouring) meta-granitoid units and granitoid plutons. **(a)** *P-T* diagram showing the estimated metamorphic conditions of shear zone nucleation in meta-granitoid (blue rectangles) and granitoid plutons (orange rectangles) from selected case studies. Legend: (1) (Ramsay and Allison, 1979); (2) Mont Blanc (Guermani and Pennacchioni, 1998); (3a) Neves shear zones, regional metamorphism (Mancktelow and

617 Pennacchioni, 2005); (3b) Neves shear zones, nucleation of precursor (Leydier et al., 2019); (4)
618 Gotthard massif – Fibbia meta-granite (Oliot et al., 2010, 2014); (5a) Gran Paradiso, regional
619 metamorphism (Menegon and Pennacchioni, 2010); (5b-c) Gran Paradiso, single samples of localised
620 shear zones (samples GPP2 and GPP5, respectively, from Rosenbaum et al., 2012); (6) Aar massif –
621 Grimsel granodiorite (Goncalves et al., 2012; Wehrens et al., 2016); (7) Suretta nappe – Roffna
622 rhyolite (Goncalves et al., 2016); (8a) Adamello and Sierra Nevada shear zones (Ceccato et al., 2020);
623 (8b) Sierra Nevada (Nevitt et al., 2017); (9) Serifos granodiorite (Tschegg and Grasemann, 2009);
624 (10) Capanne pluton, Elba Island (Smith et al., 2011); (11) Bergell pluton (Guastoni et al., 2014);
625 (12a) Rieserferner mylonites on Ep-veins (Ceccato et al., 2020); (12b) Rieserferner high-temperature
626 sheared joints and mylonites (Ceccato and Pennacchioni, 2018). Mineral abbreviations from Whitney
627 and Evans (2010). **(b)** *P-T* phase diagram section computed for an average meta-granodiorite
628 composition from the Neves Lake area, Eastern Alps (see Leydier et al., 2019). The dashed rectangle
629 represents the *P-T* conditions area shown in detail in (c). **(c)** Phase diagram section computed as in
630 (b), showing in detail the boundaries between greenschists and amphibolite facies for the meta-
631 granitoid rock. This boundary is defined by a series of univariant in- and out-reactions which assist
632 strain localisation and shear zone formation in granitoid rocks. **(d)** *T*-M_{H2O} phase diagram section
633 showing the phase relationships computed at different H_2O content (M_{H2O}). The phase fields located
634 on the right side of the H_2O-in phase boundary (black dashed curve) corresponds to the same H_2O-
635 saturated assemblage as those observed in the *P-T* section (b-c).

636 **Figure 4**. *T-X* diagrams and mass-transfer. See text for explanation.

637 **Figure 5**. Microstructures and rheology. Subscripts indicate either the magmatic ($_1$) or
638 recrystallised/metamorphic ($_2$) origin of mineral phases. **(a)** Backscatter electron (BSE) image of a
639 Kfs porphyroclast system in a mylonite from the Rieserferner pluton (modified after Ceccato et al.,
640 2018). The microstructure includes the development of myrmekite (Myrm) from Kfs_1, which lead to
641 both grain size reduction and phase mixing, producing fine aggregates of Pl_2 + Qz_2. Note the Kfs_2

642 tails on Kfs_1 porphyroclasts, suggesting the occurrence of dissolution-precipitation processes and the
643 chemical stability of Kfs. Other metamorphic reactions concur to the productions of fine-grained
644 aggregates of Pl_2 + Ep + Ms + Bt. (b) Microstructure of an orthogneiss (low-strain stage of a large
645 scale shear zone from the Fibbia meta-granite, Oliot et al., 2014) showing the occurrence of fine-
646 grained layers of Ab_2 + Pl_2 derived from Pl_1 breakdown and neo-crystallisation warping around layers
647 of dynamically recrystallised Qz_2 (modified from Fig. 3f of Oliot et al., 2014). **(c)** Log-Log
648 differential stress vs. strain rate diagram showing the rheological curves computed for the
649 deformation at 450 °C of quartz (Qz, red curve), a granitoid rock in which Qz + Pl deform by
650 dislocation creep only (GSI, blue curve), and a fine-grained aggregate of Pl_2 + Qz_2 deforming by
651 diffusion creep (GSS) only (green curve) (redrawn from Ceccato et al., 2018). The fine-grained Pl_2 +
652 Qz_2 aggregate dominated by GSS creep mechanisms is several orders of magnitude weaker than both
653 pure quartz and the Qz + Pl granitoid rock. **(d)** Log-Log grain size vs. differential stress diagram
654 showing the contoured curves for strain rate computed for quartz at 450 °C from the combination of
655 flow laws for dislocation creep (GSI) and diffusion creep (GSS) (see Ceccato et al., 2018 for more
656 details on the adopted flow laws and computation). Each contour line is marked by the Log_{10} value
657 of the strain rate. The horizontal arrows indicate the effects on quartz microstructure and rheology
658 during different processes of grain-size reduction: grain-size reduction by dynamic recrystallization
659 (grey arrow, GSR) does not lead to any significant softening, shown by the similar strain rate
660 conditions at which the white star and the grey star fall (at constant differential stress). Grain-size
661 reduction by phase mixing (orange arrow, PM) may lead to effective softening, shown by the
662 increased strain rate at which the orange star resides. The red curve represents the paleopiezometric
663 relationship defined by Cross et al. (2017).

664 **Figure 6**. Sketch of the fabric evolution and microstructural processes within a shear zone with
665 increasing shear strain. **(a)** Sketch of the microstructural evolution within the shear zone. (See the
666 main text for explanation). **(b)** Sketch of grain-boundary sliding in equigranular Pl + Qz aggregates,
667 showing also the nucleation of Kfs + Bt in the developed dynamic porosity. The red arrows indicate

668 the expulsion of fluids triggered by the mechanical contrast between the GSS creep-dominated Pl +
669 Qz aggregate and the surrounding host rock (dominated by GSI-dislocation creep). The blue arrows
670 represent the inward fluid flux triggered by the development of dynamic porosity during grain-
671 boundary sliding.

672

References

Airaghi, L., Dubacq, B., Verlaguet, A., Bourdelle, F., Bellahsen, N., Gloter, A., 2020. From static alteration to mylonitization: a nano- to micrometric study of chloritization in granitoids with implications for equilibrium and percolation length scales. Contributions to Mineralogy and Petrology 175, 1–25. https://doi.org/10.1007/S00410-020-01749-2

Austrheim, H., 1987. Eclogitization of lower crustal granulites by fluid migration through shear zones. Earth and Planetary Science Letters 81, 221–232. https://doi.org/10.1016/0012-821X(87)90158-0

Barnes, J. D., Selverstone, J., Sharp, Z. D., 2004. Interactions between serpentinite devolatilization, metasomatism and strike-slip strain localization during deep-crustal shearing in the Eastern Alps. Journal of Metamorphic Geology, 22(4), 283-300. https://doi.org/10.1111/j.1525-1314.2004.00514.x

Bestmann, M., Pennacchioni, G., 2015. Ti distribution in quartz across a heterogeneous shear zone within a granodiorite: The effect of deformation mechanism and strain on Ti resetting. Lithos. https://doi.org/10.1016/j.lithos.2015.03.009

Bras, E., Baïsset, M., Yamato, P., Labrousse, L., 2021. Transient weakening during the granulite to eclogite transformation within hydrous shear zones (Holsnøy, Norway). Tectonophysics 229026. https://doi.org/10.1016/J.TECTO.2021.229026

Bürgmann, R., Pollard, D.D., 1994. Strain accommodation about strike-slip fault discontinuities in granitic rock under brittle-to-ductile conditions. Journal of Structural Geology 16, 1655–1674. https://doi.org/10.1016/0191-8141(94)90133-3

Carreras, J., Czeck, D. M., Druguet, E., Hudleston, P. J., 2010. Structure and development of an anastomosing network of ductile shear zones. Journal of Structural Geology, 32(5), 656-666. https://doi.org/10.1016/j.jsg.2010.03.013

Ceccato, A., Goncalves, P., Pennacchioni, G., 2020. Temperature, fluid content and rheology of localized ductile shear zones in subsolidus cooling plutons. Journal of Metamorphic Geology 38, 881–903. https://doi.org/10.1111/jmg.12553

Ceccato, A., Menegon, L., Hansen, L. N., 2022. Strength of dry and wet quartz in the low-temperature plasticity regime: Insights from nanoindentation. Geophysical Research Letters, 49(2), e2021GL094633. https://doi.org/10.1029/2021GL094633Ceccato, A., Menegon, L., Pennacchioni, G., Morales, L.F.G., 2018. Myrmekite and strain weakening in granitoid mylonites. Solid Earth. https://doi.org/10.5194/se-9-1399-2018

Ceccato, A., Pennacchioni, G., 2018. Structural evolution of the Rieserferner pluton in the framework of the Oligo-Miocene tectonics of the Eastern Alps. Journal of Structural Geology 116. https://doi.org/10.1016/j.jsg.2018.08.004

Ceccato, A., Pennacchioni, G., Menegon, L., Bestmann, M., 2017. Crystallographic control and texture inheritance during mylonitization of coarse grained quartz veins. Lithos. https://doi.org/10.1016/j.lithos.2017.08.005

Cesare, B., Poletti, E., Boiron, M. C., Cathelineau, M., 2001. Alpine metamorphism and veining in the Zentralgneis Complex of the SW Tauern Window: a model of fluid–rock interactions based on fluid inclusions. Tectonophysics, 336(1-4), 121-136. https://doi.org/10.1016/S0040-1951(01)00097-X

716 Christiansen, P.P., Pollard, D.D., 1997. Nucleation, growth and structural development of mylonitic
717 shear zones in granitic rock. Journal of Structural Geology 19, 1159–1172.
718 https://doi.org/10.1016/S0191-8141(97)00025-4

719 Cisneros-Lazaro, D. G., Miller, J. A., Baumgartner, L. P., 2019. Role of myrmekite and associated
720 deformation fabrics in controlling development of granitic mylonites in the Pofadder Shear Zone
721 of southern Namibia. Contributions to Mineralogy and Petrology, 174(3), 1-20.
722 https://doi.org/10.1007/s00410-019-1555-9

723 Connolly, J.A.D., 2005. Computation of phase equilibria by linear programming: A tool for
724 geodynamic modeling and its application to subduction zone decarbonation. Earth and Planetary
725 Science Letters. https://doi.org/10.1016/j.epsl.2005.04.033

726 Cross, A.J., Ellis, S., Prior, D.J., 2015. A phenomenological numerical approach for investigating
727 grain size evolution in ductiley deforming rocks. Journal of Structural Geology 76, 22–34.
728 https://doi.org/10.1016/J.JSG.2015.04.001

729 Cross, A.J., Prior, D.J., Stipp, M., Kidder, S., 2017. The recrystallized grain size piezometer for
730 quartz: An EBSD-based calibration. Geophysical Research Letters.
731 https://doi.org/10.1002/2017GL073836

732 Cross, A. J., Skemer, P., 2017. Ultramylonite generation via phase mixing in high-strain experiments.
733 Journal of Geophysical Research: Solid Earth, 122(3), 1744-1759.
734 https://doi.org/10.1002/2016JB013801

735 Cross, A.J., Skemer, P., 2019. Rates of Dynamic Recrystallization in Geologic Materials. Journal of
736 Geophysical Research: Solid Earth 124, 1324–1342. https://doi.org/10.1029/2018JB016201

737 De Bresser, J., Ter Heege, J., Spiers, C., 2001. Grain size reduction by dynamic recrystallization: can
738 it result in major rheological weakening? International Journal of Earth Sciences 2001 90:1 90,
739 28–45. https://doi.org/10.1007/S005310000149

740 Diener, J. F., Fagereng, Å., Thomas, S. A., 2016. Mid-crustal shear zone development under
741 retrograde conditions: pressure–temperature–fluid constraints from the Kuckaus Mylonite Zone,
742 Namibia. Solid Earth, 7(5), 1331-1347. https://doi.org/10.5194/se-7-1331-2016

743 Döhmann, M. J. E. A., Brune, S., Nardini, L., Rybacki, E., Dresen, G. (2019). Strain localization and
744 weakening processes in viscously deforming rocks: Numerical modeling based on laboratory
745 torsion experiments. Journal of Geophysical Research: Solid Earth, 124(1), 1120-1137.
746 https://doi.org/10.1029/2018JB016917

747 Duretz, T., Schmalholz, S. M., Podladchikov, Y. Y., Yuen, D. A., 2014. Physics-controlled thickness
748 of shear zones caused by viscous heating: Implications for crustal shear localization.
749 Geophysical Research Letters, 41(14), 4904-4911. https://doi.org/10.1002/2014GL060438

750 Finch, M.A., Weinberg, R.F., Hunter, N.J.R., 2016. Water loss and the origin of thick ultramylonites.
751 Geology. https://doi.org/10.1130/G37972.1

752 Fitz Gerald, J.D., Stünitz, H., 1993. Deformation of granitoids at low metamorphic grade. I: Reactions
753 and grain size reduction. Tectonophysics. https://doi.org/10.1016/0040-1951(93)90163-E

754 Fleitout, L., Froidevaux, C., 1980. Thermal and mechanical evolution of shear zones. Journal of
755 Structural Geology 2, 159–164. https://doi.org/10.1016/0191-8141(80)90046-2

756 Fossen, H., Cavalcante, G.C.G., 2017. Shear zones – A review. Earth-Science Reviews 171, 434–
757 455. https://doi.org/10.1016/j.earscirev.2017.05.002

758 Fourcade, S., Marquer, D., Javoy, M., 1989. $^{18}O^{16}O$ variations and fluid circulation in a deep shear

759 zone: the case of the Alpine ultramylonites from the Aar massif (Central Alps, Switzerland).
760 Chemical geology, 77(2), 119-131. https://doi.org/10.1016/0009-2541(89)90137-X

761 Früh-Green, G. L. (1994). Interdependence of deformation, fluid infiltration and reaction progress
762 recorded in eclogitic metagranitoids (Sesia Zone, Western Alps). Journal of Metamorphic
763 Geology, 12(3), 327-343. https://doi.org/10.1111/j.1525-1314.1994.tb00026.x

764 Fusseis, F., Handy, M.R., 2008. Micromechanisms of shear zone propagation at the brittle-viscous
765 transition. Journal of Structural Geology. https://doi.org/10.1016/j.jsg.2008.06.005

766 Fusseis, F., Handy, M.R., Schrank, C., 2006. Networking of shear zones at the brittle-to-viscous
767 transition (Cap de Creus, NE Spain). Journal of Structural Geology 28, 1228–1243.
768 https://doi.org/10.1016/j.jsg.2006.03.022

769 Fusseis, F., Regenauer-Lieb, K., Liu, J., Hough, R.M., De Carlo, F., 2009. Creep cavitation can
770 establish a dynamic granular fluid pump in ductile shear zones. Nature.
771 https://doi.org/10.1038/nature08051

772 Gapais, D., 1989. Shear structures within deformed granites: mechanical and thermal indicators.
773 Geology. https://doi.org/10.1130/0091-7613(1989)017<1144:SSWDGM>2.3.CO;2

774 Gardner, R., Piazolo, S., Evans, L., Daczko, N., 2017. Patterns of strain localization in heterogeneous,
775 polycrystalline rocks–a numerical perspective. Earth and Planetary Science Letters, 463, 253-
776 265. https://doi.org/10.1016/j.epsl.2017.01.039

777 Gerbi, C., Culshaw, N., Marsh, J., 2010. Magnitude of weakening during crustal-scale shear zone
778 development. Journal of Structural Geology 32, 107–117.
779 https://doi.org/10.1016/j.jsg.2009.10.002

780 Gerbi, C., Johnson, S. E., Shulman, D., Klepeis, K., 2016. Influence of microscale weak zones on
781 bulk strength. Geochemistry, Geophysics, Geosystems, 17(10), 4064-4077.
782 https://doi.org/10.1002/2016GC006551

783 Getsinger, A. J., Hirth, G., Stünitz, H., Goergen, E. T., 2013. Influence of water on rheology and
784 strain localization in the lower continental crust. Geochemistry, Geophysics, Geosystems, 14(7),
785 2247-2264. https://doi.org/10.1002/ggge.20148

786 Gilgannon, J., Fusseis, F., Menegon, L., Regenauer-Lieb, K., Buckman, J., 2017. Hierarchical creep
787 cavity formation in an ultramylonite and implications for phase mixing. Solid Earth.
788 https://doi.org/10.5194/se-8-1193-2017

789 Gilgannon, J., Poulet, T., Berger, A., Barnhoorn, A., Herwegh, M., 2020. Dynamic Recrystallization
790 Can Produce Porosity in Shear Zones. Geophysical Research Letters 47, 1–10.
791 https://doi.org/10.1029/2019GL086172

792 Gilgannon, J., Waldvogel, M., Poulet, T., Fusseis, F., Berger, A., Barnhoorn, A., Herwegh, M., 2021.
793 Experimental evidence that viscous shear zones generate periodic pore sheets. Solid Earth 12,
794 405–420. https://doi.org/10.5194/se-12-405-2021

795 Goncalves, P., Oliot, E., Marquer, D., Connolly, J.A.D., 2012. Role of chemical processes on shear
796 zone formation: An example from the grimsel metagranodiorite (Aar massif, Central Alps).
797 Journal of Metamorphic Geology. https://doi.org/10.1111/j.1525-1314.2012.00991.x

798 Goncalves, P., Poilvet, J.C., Oliot, E., Trap, P., Marquer, D., 2016. How does shear zone nucleate?
799 An example from the Suretta nappe (Swiss Eastern Alps). Journal of Structural Geology.
800 https://doi.org/10.1016/j.jsg.2016.02.015

801 Guastoni, A., Pennacchioni, G., Pozzi, G., Fioretti, A.M., Walter, J.M., 2014. Tertiary pegmatite dikes

of the Central alps. Canadian Mineralogist 52, 191–219. https://doi.org/10.3749/canmin.52.2.191

Guermani, A., Pennacchioni, G., 1998. Brittle precursors of plastic deformation in a granite: An example from the Mont Blanc massif (Helvetic, western Alps). Journal of Structural Geology. https://doi.org/10.1016/S0191-8141(97)00080-1

Gueydan, F., Leroy, Y.M., Jolivet, L., Agard, P., 2003. Analysis of continental midcrustal strain localization induced by microfracturing and reaction-softening. Journal of Geophysical Research: Solid Earth 108, 2064. https://doi.org/10.1029/2001JB000611

Handy, M.R., 1990. The solid-state flow of polymineralic rocks. Journal of Geophysical Research 95, 8647–8661. https://doi.org/10.1029/JB095iB06p08647

Herwegh, M., Linckens, J., Ebert, A., Berger, A., Brodhag, S.H., 2011. The role of second phases for controlling microstructural evolution in polymineralic rocks: A review. Journal of Structural Geology 33, 1728–1750. https://doi.org/10.1016/J.JSG.2011.08.011

Hippertt, J.F., 1998. Breakdown of feldspar, volume gain and lateral mass transfer during mylonitization of granitoid in a low metamorphic grade shear zone. Journal of Structural Geology 20, 175–193. https://doi.org/10.1016/S0191-8141(97)00083-7

Hippertt, J. F., Hongn, F. D., 1998. Deformation mechanisms in the mylonite/ultramylonite transition. Journal of Structural Geology, 20(11), 1435-1448. https://doi.org/10.1016/S0191-8141(98)00047-9

Hobbs, B.E., Ord, A., Regenauer-Lieb, K., 2011. The thermodynamics of deformed metamorphic rocks: A review. Journal of Structural Geology 33, 758–818. https://doi.org/10.1016/j.jsg.2011.01.013

Hobbs, B.E., Ord, A., Spalla, M.I., Gosso, G., Zucali, M., 2010. The interaction of deformation and metamorphic reactions. Geological Society Special Publication 332, 189–223. https://doi.org/10.1144/SP332.12

Holland, T.J.B., Powell, R., 2011. An improved and extended internally consistent thermodynamic dataset for phases of petrological interest, involving a new equation of state for solids. Journal of Metamorphic Geology 29, 333–383. https://doi.org/10.1111/J.1525-1314.2010.00923.X

Holyoke, C.W., Tullis, J., 2006. The interaction between reaction and deformation: An experimental study using a biotite + plagioclase + quartz gneiss. Journal of Metamorphic Geology 24, 743–762. https://doi.org/10.1111/j.1525-1314.2006.00666.x

Huet, B., Yamato, P., Grasemann, B., 2014. The Minimized Power Geometric model: An analytical mixing model for calculating polyphase rock viscosities consistent with experimental data. Journal of Geophysical Research: Solid Earth 119, 3897–3924. https://doi.org/10.1002/2013JB010453

Hull, J., 1988. Thickness-displacement relationships for deformation zone. Journal of Structural Geology 10, 431–435. https://doi.org/10.1016/0191-8141(88)90020-X

Ingles, J., Lamouroux, C., Soula, J.C., Guerrero, N., Debat, P., 1999. Nucleation of ductile shear zones in a granodiorite under greenschist facies conditions, Neouvielle massif, Pyrenees, France. Journal of Structural Geology 21, 555–576. https://doi.org/10.1016/S0191-8141(99)00042-5

Kaatz, L., Zertani, S., Moulas, E., John, T., Labrousse, L., Schmalholz, S.M., Andersen, T.B., 2021. Widening of hydrous shear zones during incipient eclogitization of metastable dry and rigid lower crust – Holsnøy, Western Norway. Tectonics. https://doi.org/10.1029/2020TC006572

Keller, L. M., Abart, R., Stünitz, H., De Capitani, C., 2004. Deformation, mass transfer and mineral reactions in an eclogite facies shear zone in a polymetamorphic metapelite (Monte Rosa nappe, western Alps). Journal of Metamorphic Geology, 22(2), 97-118. https://doi.org/10.1111/j.1525-1314.2004.00500.x

Kilian, R., Heilbronner, R., Stünitz, H., 2011. Quartz grain size reduction in a granitoid rock and the transition from dislocation to diffusion creep. Journal of Structural Geology. https://doi.org/10.1016/j.jsg.2011.05.004

Kiss, D., Podladchikov, Y., Duretz, T., Schmalholz, S.M., 2019. Spontaneous generation of ductile shear zones by thermal softening: Localization criterion, 1D to 3D modelling and application to the lithosphere. Earth and Planetary Science Letters 519, 284–296. https://doi.org/10.1016/j.epsl.2019.05.026

Korzhiniskii, D. S., 1970. Theory of Metasomatie Zoning. Oxford: Oxford University Press.

Kronenberg, A.K., Ashley, K.T., Francsis, M.K., Holyoke, C.W., Jezek, L., Kronenberg, J.A., Law, R.D., Thomas, J.B., 2020. Water loss during dynamic recrystallization of Moine thrust quartzites, northwest Scotland. Geology 48, 557–561. https://doi.org/10.1130/G47041.1

Kronenberg, A.K., Wolf, G.H., 1990. Fourier transform infrared spectroscopy determinations of intragranular water content in quartz-bearing rocks: implications for hydrolytic weakening in the laboratory and within the earth. Tectonophysics 172, 255–271. https://doi.org/10.1016/0040-1951(90)90034-6

Lamouroux, C., Debat, P., Inglés, J., Guerrero, N., Sirieys, P., Soula, J.C., 1994. Rheological properties of rock inferred from the geometry and microstructures in two natural shear zones. Mechanics of Materials 18, 79–87. https://doi.org/10.1016/0167-6636(94)90018-3

Lee, A. L., Stünitz, H., Soret, M., Battisti, M. A., 2022. Dissolution precipitation creep as a process for the strain localisation in mafic rocks. Journal of Structural Geology, 104505. https://doi.org/10.1016/j.jsg.2021.104505

Leydier, T., Goncalves, P., Lanari, P., Oliot, E., 2019. On the petrology of brittle precursors of shear zones – An expression of concomitant brittle deformation and fluid–rock interactions in the 'ductile' continental crust? Journal of Metamorphic Geology. https://doi.org/10.1111/jmg.12504

Macente, A., Fusseis, F., Menegon, L., Xiao, X., John, T., 2017. The strain-dependent spatial evolution of garnet in a high-P ductile shear zone from the Western Gneiss Region (Norway): a synchrotron X-ray microtomography study. Journal of Metamorphic Geology, 35(5), 565-583. https://doi.org/10.1111/jmg.12245

Mancktelow, N.S., 2002. Finite-element modelling of shear zone development in viscoelastic materials and its implications for localisation of partial melting. Journal of Structural Geology 24, 1045–1053. https://doi.org/10.1016/S0191-8141(01)00090-6

Mancktelow, N. S., 2006. How ductile are ductile shear zones?. Geology, 34(5), 345-348. https://doi.org/10.1130/G22260.1

Mancktelow, N.S., Pennacchioni, G., 2013. Late magmatic healed fractures in granitoids and their influence on subsequent solid-state deformation. Journal of Structural Geology. https://doi.org/10.1016/j.jsg.2013.09.006

Mancktelow, N.S., Pennacchioni, G., 2005. The control of precursor brittle fracture and fluid-rock interaction on the development of single and paired ductile shear zones. Journal of Structural Geology. https://doi.org/10.1016/j.jsg.2004.12.001

Mancktelow, N.S., Pennacchioni, G., 2004. The influence of grain boundary fluids on the microstructure of quartz-feldspar mylonites. Journal of Structural Geology. https://doi.org/10.1016/S0191-8141(03)00081-6

Mansard, N., Raimbourg, H., Augier, R., Précigout, J., Le Breton, N., 2018. Large-scale strain localization induced by phase nucleation in mid-crustal granitoids of the south Armorican massif. Tectonophysics, 745, 46-65. https://doi.org/10.1016/j.tecto.2018.07.022

Marquer, D., Gapais, D., Capdevila, R., 1985. Comportement chimique et orthogneissification d'une granodiorite en facies schistes verts (Massif de l'Aar, Alpes Centrales). Bulletin de minéralogie, 108(2), 209-221.

McCaig, A.M., 1984. Fluid-rock interaction in some shear zones from the Pyrenees. Journal of Metamorphic Geology 2, 129–141. https://doi.org/10.1111/J.1525-1314.1984.TB00292.X

McCaig, A. M., Wickham, S. M., Taylor, H. P., 1990. Deep fluid circulation in alpine shear zones, Pyrenees, France: field and oxygen isotope studies. Contributions to Mineralogy and Petrology, 106(1), 41-60. https://doi.org/10.1007/BF00306407

Means, W.D., 1995. Shear zones and rock history. Tectonophysics 247, 157–160. https://doi.org/10.1016/0040-1951(95)98214-H

Menegon, L., Fagereng, Å., 2021. Tectonic pressure gradients during viscous creep drive fluid flow and brittle failure at the base of the seismogenic zone. Geology 49, 1255–1259. https://doi.org/10.1130/G49012.1

Menegon, L., Fusseis, F., Stünitz, H., Xiao, X., 2015. Creep cavitation bands control porosity and fluid flow in lower crustal shear zones. Geology. https://doi.org/10.1130/G36307.1

Menegon, L., Pennacchioni, G., 2010. Local shear zone pattern and bulk deformation in the Gran Paradiso metagranite (NW Italian Alps). International Journal of Earth Sciences 99, 1805–1825. https://doi.org/10.1007/S00531-009-0485-6/FIGURES/15

Menegon, L., Pennacchioni, G., Heilbronner, R., Pittarello, L., 2008a. Evolution of quartz microstructure and c-axis crystallographic preferred orientation within ductilely deformed granitoids (Arolla unit, Western Alps). Journal of Structural Geology, 30(11), 1332-1347. https://doi.org/10.1016/j.jsg.2008.07.007

Menegon, L., Pennacchioni, G., Spiess, R., 2008b. Dissolution-precipitation creep of K-feldspar in mid-crustal granite mylonites. Journal of Structural Geology. https://doi.org/10.1016/j.jsg.2008.02.001

Menegon, L., Pennacchioni, G., Stünitz, H., 2006. Nucleation and growth of myrmekite during ductile shear deformation in metagranites. Journal of Metamorphic Geology. https://doi.org/10.1111/j.1525-1314.2006.00654.x

Meyer, S.E., Kaus, B.J.P., Passchier, C., 2016. Development of branching brittle and ductile shear zones: A numerical study. Geochemistry, Geophysics, Geosystems 18, 2054–2075. https://doi.org/10.1002/2016GC006793

Mittempergher, S., Dallai, L., Pennacchioni, G., Renard, F., Di Toro, G., 2014. Origin of hydrous fluids at seismogenic depth: Constraints from natural and experimental fault rocks. Earth and Planetary Science Letters, 385, 97-109. https://doi.org/10.1016/j.epsl.2013.10.027

Nardini, L., Rybacki, E., Döhmann, M. J., Morales, L. F., Brune, S., Dresen, G., 2018. High-temperature shear zone formation in Carrara marble: The effect of loading conditions. Tectonophysics, 749, 120-139. https://doi.org/10.1016/j.tecto.2018.10.022

931 Nevitt, J. M., Pollard, D. D., Warren, J. M., 2014. Evaluation of transtension and transpression within
932 contractional fault steps: Comparing kinematic and mechanical models to field data. Journal of
933 Structural Geology, 60, 55-69. https://doi.org/10.1016/j.jsg.2013.12.011

934 Nevitt, J. M., Pollard, D. D., 2017. Impacts of off-fault plasticity on fault slip and interaction at the
935 base of the seismogenic zone. Geophysical Research Letters, 44(4), 1714-1723.
936 https://doi.org/10.1002/2016GL071688

937 Nevitt, J.M., Warren, J.M., Kidder, S., Pollard, D.D., 2017. Comparison of thermal modeling,
938 microstructural analysis, and Ti-in-quartz thermobarometry to constrain the thermal history of a
939 cooling pluton during deformation in the Mount Abbot Quadrangle, CA. Geochemistry,
940 Geophysics, Geosystems. https://doi.org/10.1002/2016GC006655

941 Oliot, E., Goncalves, P., Marquer, D., 2010. Role of plagioclase and reaction softening in a
942 metagranite shear zone at mid-crustal conditions (Gotthard Massif, Swiss Central Alps). Journal
943 of Metamorphic Geology. https://doi.org/10.1111/j.1525-1314.2010.00897.x

944 Oliot, E., Goncalves, P., Schulmann, K., Marquer, D., Lexa, O., 2014. Mid-crustal shear zone
945 formation in granitic rocks: Constraints from quantitative textural and crystallographic preferred
946 orientations analyses. Tectonophysics 612–613, 63–80.
947 https://doi.org/10.1016/j.tecto.2013.11.032

948 Oriolo, S., Wemmer, K., Oyhantçabal, P., Fossen, H., Schulz, B., Siegesmund, S., 2018.
949 Geochronology of shear zones – A review. Earth-Science Reviews 185, 665–683.
950 https://doi.org/10.1016/j.earscirev.2018.07.007

951 Passchier, C. W., 1982. Pseudotachylyte and the development of ultramylonite bands in the Saint-
952 Barthelemy Massif, French Pyrenees. Journal of Structural Geology, 4(1), 69-79. DOI:
953 10.1016/0191-8141(82)90008-6

954 Pennacchioni, G., 2005. Control of the geometry of precursor brittle structures on the type of ductile
955 shear zone in the Adamello tonalites, Southern Alps (Italy). Journal of Structural Geology.
956 https://doi.org/10.1016/j.jsg.2004.11.008

957 Pennacchioni, G., 1996. Progressive eclogitization under fluid-present conditions of pre-Alpine mafic
958 granulites in the Austroalpine Mt Emilius Klippe (Italian Western Alps). Journal of Structural
959 Geology. https://doi.org/10.1016/S0191-8141(96)80023-X

960 Pennacchioni, G., Cesare, B., 1997. Ductile-brittle transition in pre-Alpine amphibolite facies
961 mylonites during evolution from water-present to water-deficient conditions (Mont Mary nappe,
962 Italian Western Alps). Journal of Metamorphic Geology. https://doi.org/10.1111/j.1525-
963 1314.1997.00055.x

964 Pennacchioni, G., Mancktelow, N.S., 2018. Small-scale ductile shear zones: Neither extending, nor
965 thickening, nor narrowing., Earth-Science Reviews.
966 https://doi.org/10.1016/j.earscirev.2018.06.004

967 Pennacchioni, G., Mancktelow, N.S., 2007. Nucleation and initial growth of a shear zone network
968 within compositionally and structurally heterogeneous granitoids under amphibolite facies
969 conditions. Journal of Structural Geology. https://doi.org/10.1016/j.jsg.2007.06.002

970 Pennacchioni, G., Menegon, L., Leiss, B., Nestola, F., Bromiley, G., 2010. Development of
971 crystallographic preferred orientation and microstructure during plastic deformation of natural
972 coarse-grained quartz veins. Journal of Geophysical Research: Solid Earth.
973 https://doi.org/10.1029/2010JB007674

974 Pennacchioni, G., Zucchi, E., 2013. High temperature fracturing and ductile deformation during

cooling of a pluton: The Lake Edison granodiorite (Sierra Nevada batholith, California). Journal of Structural Geology. https://doi.org/10.1016/j.jsg.2012.06.001

Platt, J.P., 2015. Rheology of two-phase systems: A microphysical and observational approach. Journal of Structural Geology 77, 213–227. https://doi.org/10.1016/j.jsg.2015.05.003

Platt, J. P., Behr, W. M., 2011a. Grainsize evolution in ductile shear zones: Implications for strain localization and the strength of the lithosphere. Journal of Structural Geology, 33(4), 537-550. https://doi.org/10.1016/j.jsg.2011.01.018

Platt, J. P., Behr, W. M., 2011b. Lithospheric shear zones as constant stress experiments. Geology, 39(2), 127-130. https://doi.org/10.1130/G31561.1

Poirier, J.P., 1980. Shear localization and shear instability in materials in the ductile field. Journal of Structural Geology 2, 135–142. https://doi.org/10.1016/0191-8141(80)90043-7

Ramsay, J.G., 1980. Shear zone geometry: A review. Journal of Structural Geology 2, 83–99. https://doi.org/10.1016/0191-8141(80)90038-3

Ramsay, J.G., Allison, I., 1979. Structural analysis of shear zones in an alpinized hercynian granite (Maggia Lappen, Pennine Zone, Central Alps). Schweiz. Miner. Petrogr. Mitt. 59, 251–279.

Ramsay, J.G., Graham, R.H., 1970. Strain variation in shear belts. Canadian Journal of Earth Sciences 7, 786–813. https://doi.org/10.1139/e70-078

Ree, J. H., Kim, H. S., Han, R., Jung, H., 2005. Grain-size reduction of feldspars by fracturing and neocrystallization in a low-grade granitic mylonite and its rheological effect. Tectonophysics, 407(3-4), 227-237. https://doi.org/10.1016/j.tecto.2005.07.010

Regenauer-Lieb, K., Yuen, D.A., 2003. Modeling shear zones in geological and planetary sciences: Solid- and fluid-thermal-mechanical approaches. Earth-Science Reviews 63, 295–349. https://doi.org/10.1016/S0012-8252(03)00038-2

Rennie, S. F., Fagereng, Å., Diener, J. F. A., 2013. Strain distribution within a km-scale, mid-crustal shear zone: the Kuckaus Mylonite Zone, Namibia. Journal of Structural Geology, 56, 57-69. https://doi.org/10.1016/j.jsg.2013.09.001

Rolland, Y., Rossi, M., 2016. Two-stage fluid flow and element transfers in shear zones during collision burial-exhumation cycle: Insights from the Mont Blanc Crystalline Massif (Western Alps). Journal of Geodynamics, 101, 88-108. https://doi.org/10.1016/j.jog.2016.03.016

Rosenbaum, G., Menegon, L., Glodny, J., Vasconcelos, P., Ring, U., Massironi, M., Thiede, D., Nasipuri, P., 2012. Dating deformation in the Gran Paradiso Massif (NW Italian Alps): Implications for the exhumation of high-pressure rocks in a collisional belt. Lithos 144–145, 130–144. https://doi.org/10.1016/J.LITHOS.2012.04.016

Rossi, M., Rolland, Y., Vidal, O., Cox, S. F., 2005. Geochemical variations and element transfer during shear-zone development and related episyenites at middle crust depths: insights from the Mont Blanc granite (French—Italian Alps). Geological Society, London, Special Publications, 245(1), 373-396. https://doi.org/10.1144/GSL.SP.2005.245.01.18

Sassier, C., Boulvais, P., Gapais, D., Capdevila, R., Diot, H., 2006. From granitoid to kyanite-bearing micaschist during fluid-assisted shearing (Ile d'Yeu, France). International Journal of Earth Sciences 95, 2–18. https://doi.org/10.1007/S00531-005-0011-4

Schrank, C. E., Boutelier, D. A., Cruden, A. R., 2008a. The analogue shear zone: From rheology to associated geometry. Journal of Structural Geology, 30(2), 177-193. https://doi.org/10.1016/j.jsg.2007.11.002

Schrank, C. E., Handy, M. R., Fusseis, F., 2008b. Multiscaling of shear zones and the evolution of the brittle- to- viscous transition in continental crust. Journal of Geophysical Research: Solid Earth, 113(B1).

Segall, P., Simpson, C., 1986. Nucleation of ductile shear zones on dilatant fractures. Geology. https://doi.org/10.1130/0091-7613(1986)14<56:NODSZO>2.0.CO;2

Shigematsu, N., 1999. Dynamic recrystallization in deformed plagioclase during progressive shear deformation. Tectonophysics 305, 437–452. https://doi.org/10.1016/S0040-1951(99)00039-6

Sibson, R.H., 1975. Generation of pseudotachylyte by ancient seismic faulting. Geophys. J. R. Astr. Soc., 43, 775-794. https://doi.org/10.1111/j.1365-246X.1975.tb06195.x

Smith, J.R., Piazolo, S., Daczko, N.R., Evans, L., 2015. The effect of pre-tectonic reaction and annealing extent on behaviour during subsequent deformation: Insights from paired shear zones in the lower crust of Fiordland, New Zealand. Journal of Metamorphic Geology 33, 557–577. https://doi.org/10.1111/jmg.12132

Smith, S.A.F., Holdsworth, R.E., Collettini, C., 2011. Interactions between low-angle normal faults and plutonism in the upper crust: Insights from the Island of Elba, Italy. GSA Bulletin 123, 329–346. https://doi.org/10.1130/B30200.1

Spruzeniece, L., Piazolo, S., 2015. Strain localization in brittle-ductile shear zones: Fluid-abundant vs. fluid-limited conditions (an example from Wyangala area, Australia). Solid Earth 6, 881–901. https://doi.org/10.5194/se-6-881-2015

Steffen, K., Selverstone, J., Brearley, A., 2001. Episodic weakening and strengthening during synmetamorphic deformation in a deep-crustal shear zone in the Alps. Geological Society, London, Special Publications, 186(1), 141-156. https://doi.org/10.1144/GSL.SP.2001.186.01.09

Stenvall, C.A., Fagereng, Å., Diener, J.F.A., 2019. Weaker Than Weakest: On the Strength of Shear Zones. Geophysical Research Letters. https://doi.org/10.1029/2019GL083388

Stenvall, C. A., Fagereng, A., Diener, J. F. A., Harris, C., Janney, P. E., 2020. Sources and effects of fluids in continental retrograde shear zones: Insights from the Kuckaus Mylonite Zone, Namibia. Geofluids, 2020. https://doi.org/10.1155/2020/3023268

Stipp, M., Stünitz, H., Heilbronner, R., Schmid, S.M., 2002. The eastern Tonale fault zone: A "natural laboratory" for crystal plastic deformation of quartz over a temperature range from 250 to 700 °C. Journal of Structural Geology. https://doi.org/10.1016/S0191-8141(02)00035-4

Stünitz, H., Fitz Gerald, J.D., 1993. Deformation of granitoids at low metamorphic grade. II: Granular flow in albite-rich mylonites. Tectonophysics. https://doi.org/10.1016/0040-1951(93)90164-F

Sullivan, W. A., Boyd, A. S., Monz, M. E., 2013. Strain localization in homogeneous granite near the brittle–ductile transition: a case study of the Kellyland fault zone, Maine, USA. Journal of Structural Geology, 56, 70-88. https://doi.org/10.1016/j.jsg.2013.09.003

Takagi, H., Goto, K., Shigematsu, N., 2000. Ultramylonite bands derived from cataclasite and pseudotachylyte in granites, northeast Japan. Journal of Structural Geology, 22(9), 1325-1339. https://doi.org/10.1016/S0191-8141(00)00034-1

Tobisch, O. T., Barton, M. D., Vernon, R. H., Paterson, S. R., 1991. Fluid-enhanced deformation: transformation of granitoids to banded mylonites, western Sierra Nevada, California, and southeastern Australia. Journal of Structural Geology, 13(10), 1137-1156.

Tokle, L., Hirth, G., 2021. Assessment of Quartz Grain Growth and the Application of the Wattmeter to Predict Quartz Recrystallized Grain Sizes. Journal of Geophysical Research: Solid Earth 126,

e2020JB021475. https://doi.org/10.1029/2020JB021475

Tschegg, C., Grasemann, B., 2009. Deformation and alteration of a granodiorite during low-angle normal faulting (Serifos, Greece). Lithosphere. https://doi.org/10.1130/L33.1

Tsurumi, J., Hosonuma, H., Kanagawa, K., 2003. Strain localization due to a positive feedback of deformation and myrmekite-forming reaction in granite and aplite mylonites along the Hatagawa Shear Zone of NE Japan. Journal of Structural Geology, 25(4), 557-574. https://doi.org/10.1016/S0191-8141(02)00048-2

Tursi, F., 2022. The key role of μH2O gradients in deciphering microstructures and mineral assemblages of mylonites: examples from the Calabria polymetamorphic terrane. Mineralogy and Petrology, 116, 1-14. https://doi.org/10.1007/s00710-021-00766-8

Tursi, F., Festa, V., Fornelli, A., Micheletti, F., Spiess, R., 2018. Syn-shearing mobility of major elements in ductile shear zones: state of the art for felsic deformed protoliths. Period. Mineral, 87, 289-308. DOI: 10.2451/2018PM811

Van Roermund, H., Lister, G. S., Williams, P. F., 1979. Progressive development of quartz fabrics in a shear zone from Monte Mucrone, Sesia-Lanzo Zone, Italian Alps. Journal of Structural Geology, 1(1), 43-52. https://doi.org/10.1016/0191-8141(79)90020-8

Viegas, G., Menegon, L., Archanjo, C., 2016. Brittle grain-size reduction of feldspar, phase mixing and strain localization in granitoids at mid-crustal conditions (Pernambuco shear zone, NE Brazil). Solid Earth. https://doi.org/10.5194/se-7-375-2016

Vitale, S., Mazzoli, S., 2008. Heterogeneous shear zone evolution: The role of shear strain hardening/softening. Journal of Structural Geology 30, 1383–1395. https://doi.org/10.1016/j.jsg.2008.07.006

Wehrens, P., Baumberger, R., Berger, A., Herwegh, M., 2017. How is strain localized in a meta-granitoid, mid-crustal basement section? Spatial distribution of deformation in the central Aar massif (Switzerland). Journal of Structural Geology, 94, 47-67. https://doi.org/10.1016/j.jsg.2016.11.004

Wehrens, P., Berger, A., Peters, M., Spillmann, T., Herwegh, M., 2016. Deformation at the frictional-viscous transition: Evidence for cycles of fluid-assisted embrittlement and ductile deformation in the granitoid crust. Tectonophysics, 693, 66-84. https://doi.org/10.1016/j.tecto.2016.10.022

White, R.W., Powell, R., Holland, T.J.B., Johnson, T.E., Green, E.C.R., 2014. New mineral activity-composition relations for thermodynamic calculations in metapelitic systems. Journal of Metamorphic Geology. https://doi.org/10.1111/jmg.12071

White, S.H., Burrows, S.E., Carreras, J., Shaw, N.D., Humphreys, F.J., 1980. On mylonites in ductile shear zones. Journal of Structural Geology 2, 175–187. https://doi.org/10.1016/0191-8141(80)90048-6

Whitney, D.L., Evans, B.W., 2010. Abbreviations for names of rock-forming minerals. American Mineralogist. https://doi.org/10.2138/am.2010.3371

Whyte, A. J., Weller, O. M., Copley, A. C., St-Onge, M. R., 2021. Quantifying water diffusivity and metamorphic reaction rates within mountain belts, and their implications for the rheology of cratons. Geochemistry, Geophysics, Geosystems, 22(11), e2021GC009988. https://doi.org/10.1029/2021GC009988

Wintsch, R. P., Yi, K., 2002. Dissolution and replacement creep: a significant deformation mechanism in mid-crustal rocks. Journal of Structural Geology, 24(6-7), 1179-1193.

https://doi.org/10.1016/S0191-8141(01)00100-6

Yardley, B. W., 1981. Effect of cooling on the water content and mechanical behavior of metamorphosed rocks. Geology, 9(9), 405-408. https://doi.org/10.1130/0091-7613(1981)9%3C405:EOCOTW%3E2.0.CO;2

Yardley, B.W.D., Valley, J.W., 1997. The petrologic case for a dry lower crust. Journal of Geophysical Research: Solid Earth. https://doi.org/10.1029/97jb00508

Figure 1

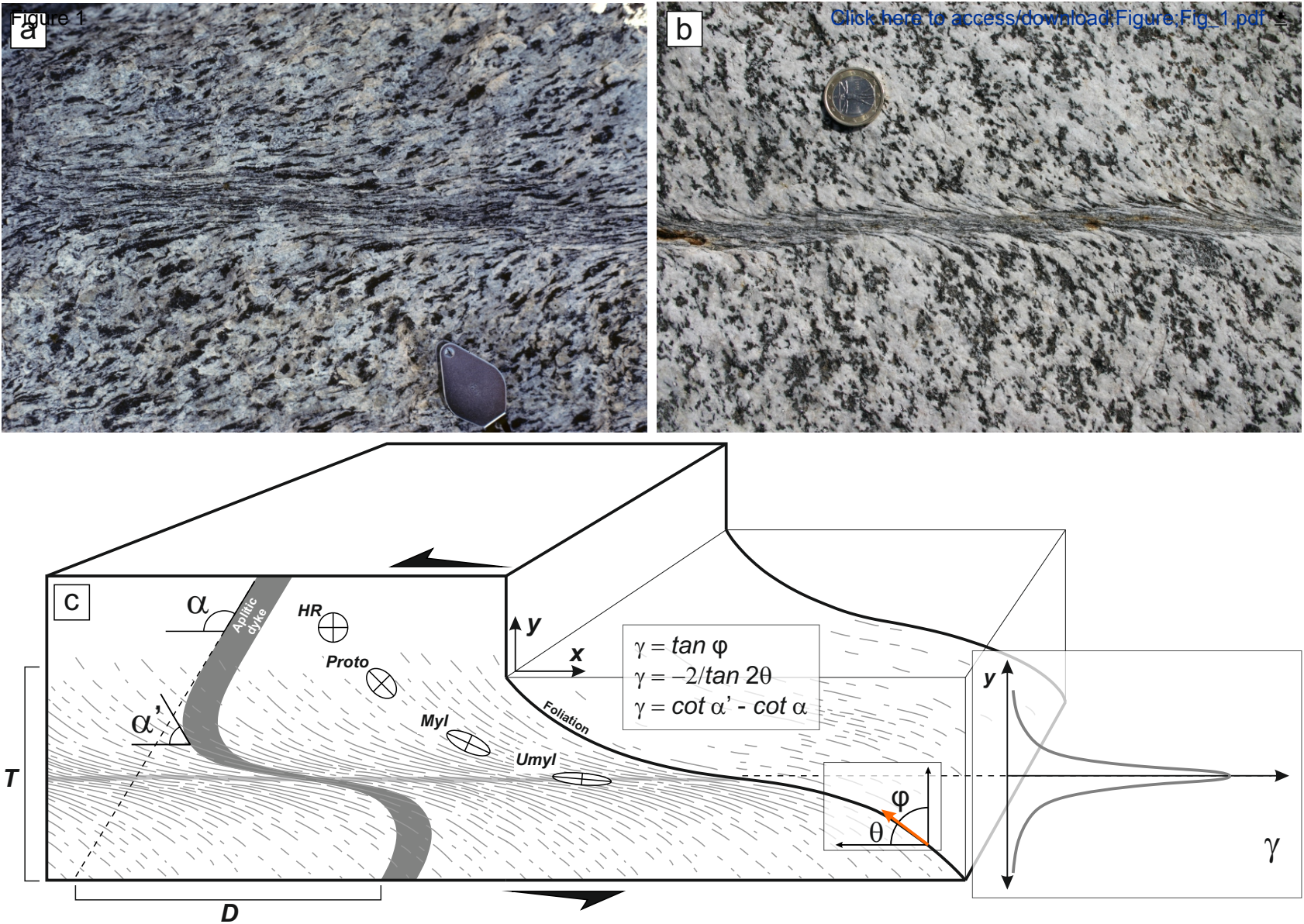

Figure 2

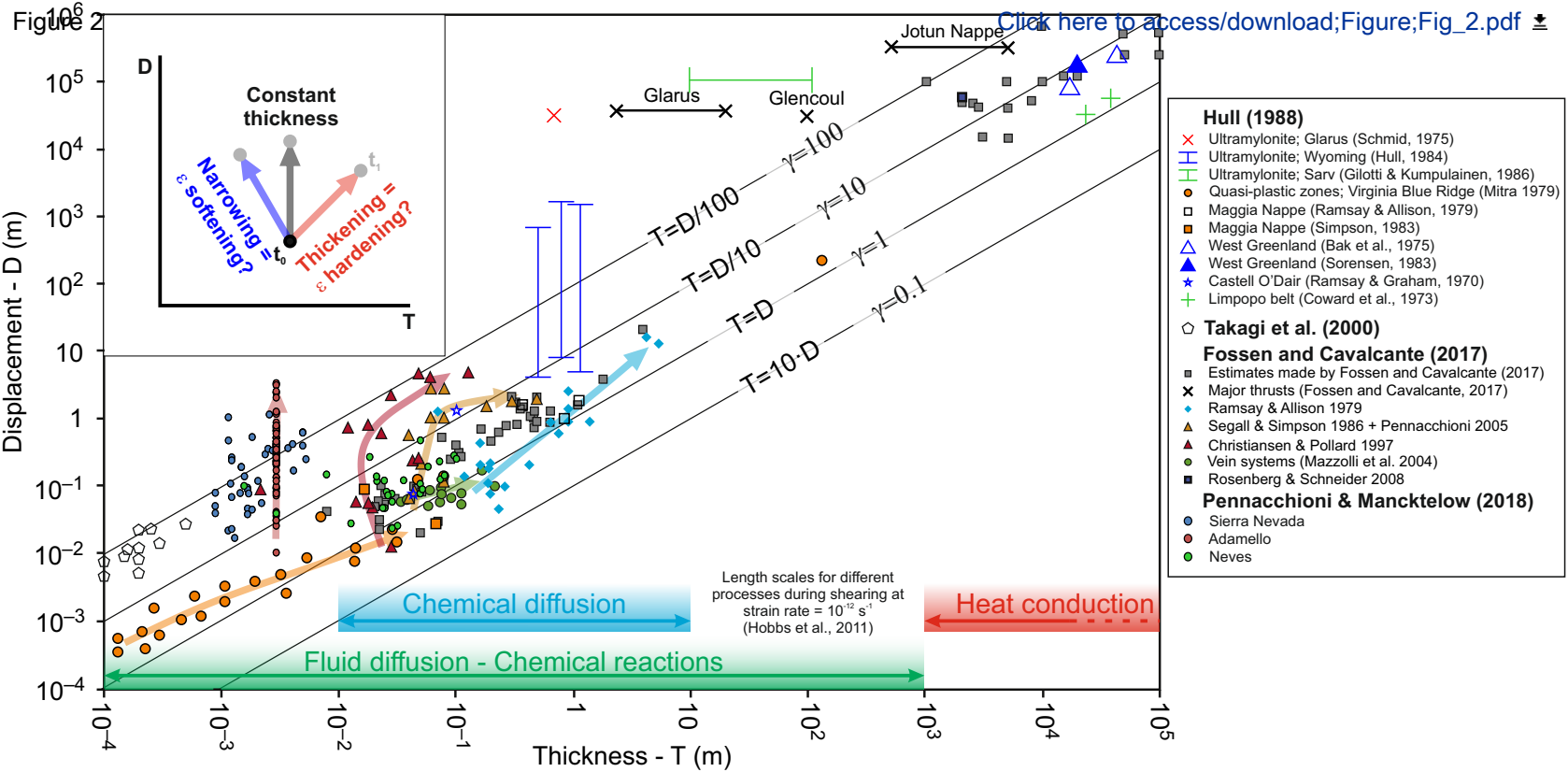

Figure 3

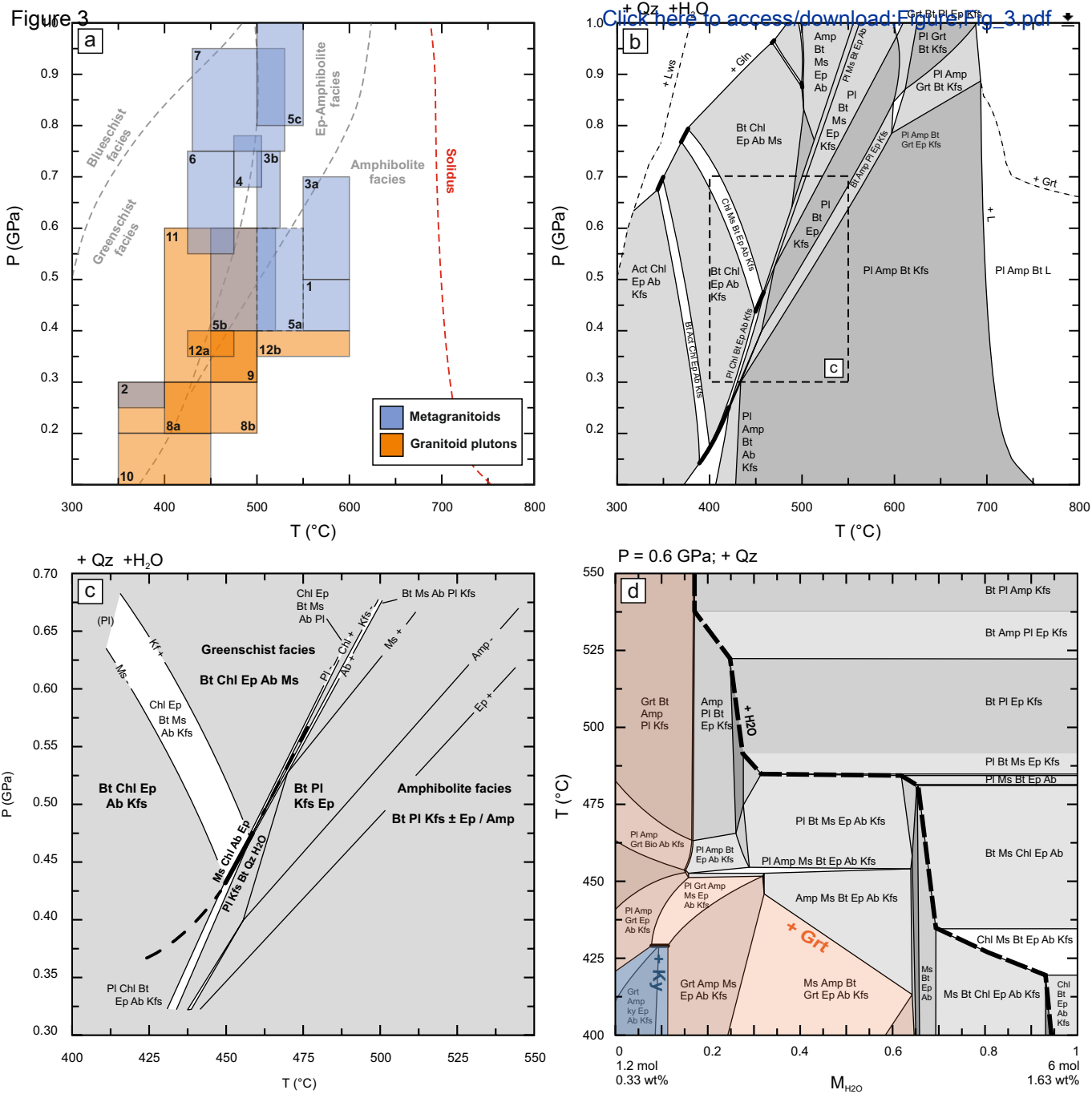

Figure 4

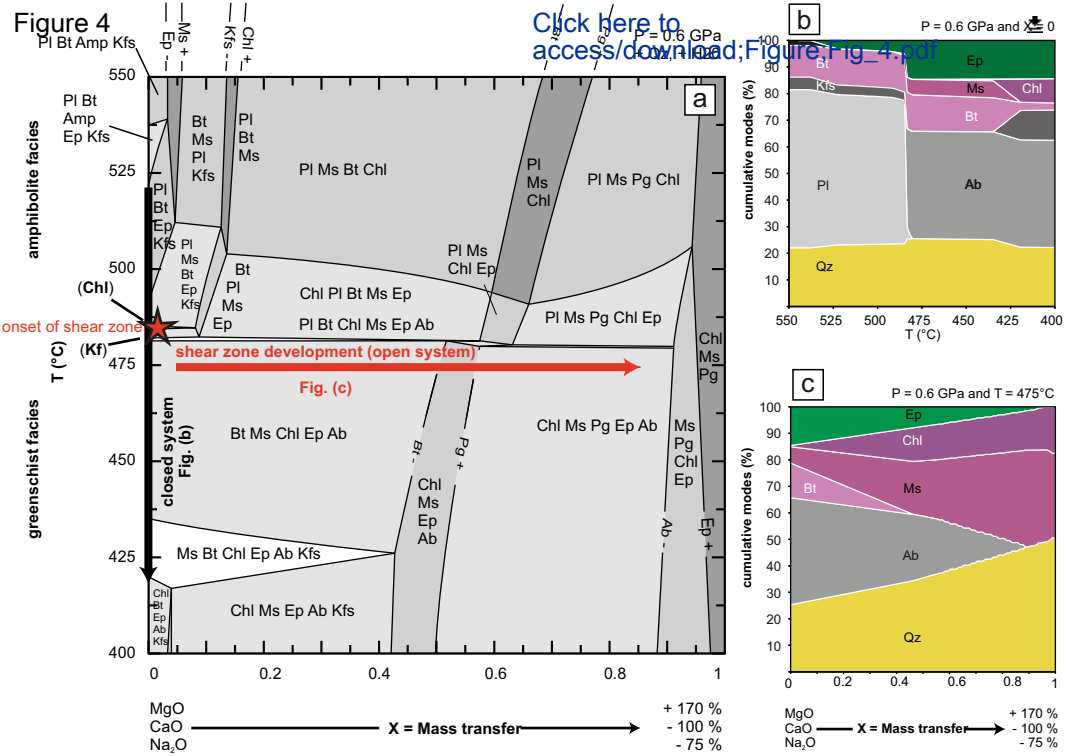

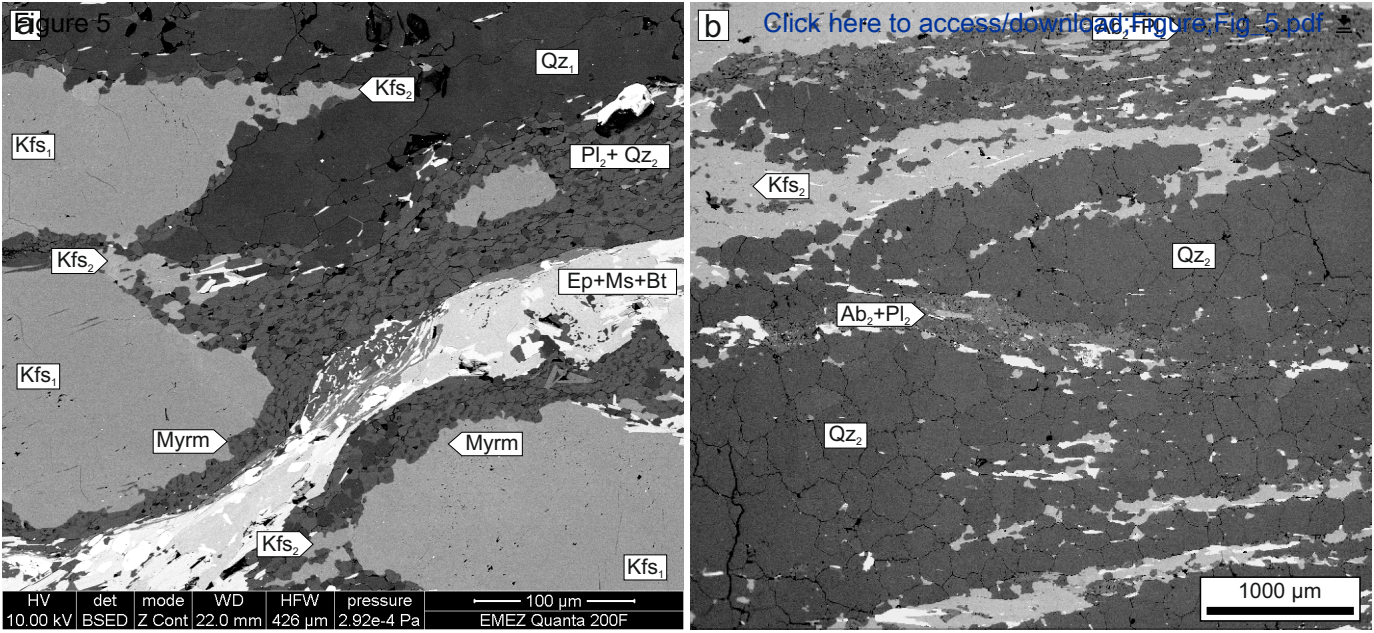

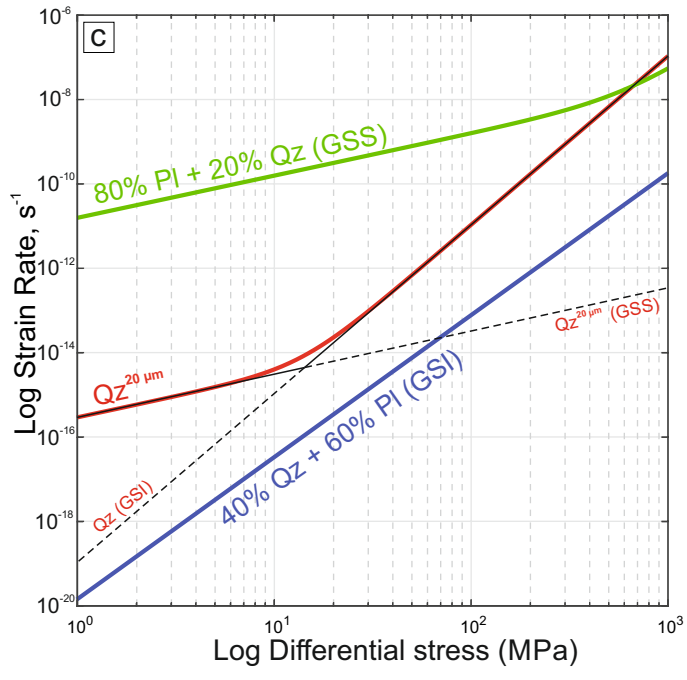

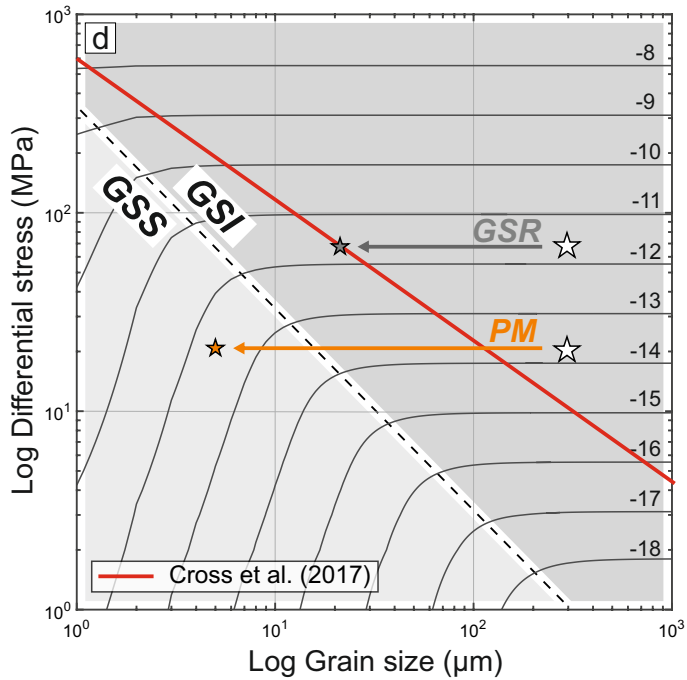

Figure 6